LunarEX

A proposal to ESA Cosmic Vision

The Moon:
A record of our past,
the next step to our future

Lead Proposer: A. Smith (UK)

Core Proposal Team (UK):
I. A. Crawford
A. J. Ball
S. J. Barber
P. Church
A. J. Coates
Y. Gao
R. A. Gowen
A. D. Griffiths
A. Phipps
T. Pike
R. Scott
S. Sheridan
M. Sweeting
D. Talboys
V. Tong
N. Wells

Supporting Proposers

Austria: G. Kargl
Germany: J. Biele, G. Klingelhoefer, L. Richter, S. Ulamec
France: M. Wieczorek
Italy: J. Chela-Flores
Ireland: S. McKenna-Lawlor
Poland: K. Seweryn, R. Wawrzaszek, J. Grygorczuk, W. Marczewski, B. Dabrowski
Russia: O. Khavroshkin
UK: J. Flannagan, M. Grande, D.A. Rothery, I.P. Wright

Industry Studies

Surrey Satellite Technology Ltd.
QinetiQ Ltd.

LunarEX – A proposal to Cosmic Vision

Executive Summary

While the surface missions to the Moon of the 1970's achieved a great deal, scientifically a great deal was also left unresolved. The recent plethora of Lunar missions (flown or proposed) reflects a resurgence in interest in the Moon, not only in its own right, but also as a record of the early solar system including the formation of the Earth. Results from recent orbiter missions have shown evidence of ice within shaddowed craters at the Lunar poles.

We propose a highly cost effective M-class Lunar mission that will place 4 or more scientifically instrumented penetrators into the Lunar surface.

LunarEX will address key issues related to the origin and evolution of planetary bodies as well as the astrobiologically important possibilities associated with polar ice. LunarEX will provide important information about:

- The size and physical state of the Lunar core
- The deep structure of the Lunar mantle
- The thickness of the farside Lunar crust
- The nature of natural Moonquakes, in particular the origin of shallow Moonquakes
- The composition and thermal evolution of the Moon's interior
- The existence, nature and origin of polar ice – exciting scientifically and key to future manned exploration of the Moon and beyond

The penetrators will be globally dispersed (unlike the Apollo missions) with landing sites on the nearside Procellarum KREEP Terrain, poles and farside, and will operate 2-5m beneath the Lunar surface for 1 year.

Each penetrator will include a suite of scientific instruments including micro-seismometers, a geochemistry package, a water/volatiles detector (for the polar penetrator(s)), a heat flow experiment, and an impact accelerometer.

For an instrument to survive an impact at 300 ms^{-1} is entirely feasible and a vast amount of resource has been devoted to such conditions within a defence context. 'Penetrators' are common-place within that sector and instrumentation is available off-the-shelf which will survive impacts of >50,000g (LunarEX expects up to 10,000g). This expertise is by no means purely empirical in nature; a very sophisticated predictive modeling capability also exists. The LunarEX project plans to tap this capability for a scientific end. Moreover, Mars 96, DS-2 and Lunar-A penetrator development programmes have overcome many key problems and demonstrated survivability in ground tests.

The penetrator delivery to the Lunar surface will take place in two stages:

- The Penetrators will be transferred to Lunar orbit as the payload of what will become a polar orbit communications relay satellite
- Release, de-orbit and descent. Each penetrator will have an attached de-orbit motor and attitude control systems (both of which are ejected before impact)

The mission is compatible with a single Soyuz-Fregat launch for a nominal 4 penetrator payload with a 30% mass contingency.

LunarEX will fill an important gap within the proposed international Lunar mission portfolio and facilitate the future scientific and ultimately manned exploration of the Moon.

1. Introduction

1.1 The Moon

The principal scientific importance of the Moon is as a recorder of geological processes active in the early history of terrestrial planets (e.g. planetary differentiation, magma ocean formation and evolution), and of the near-Earth cosmic environment (e.g. bombardment history, solar wind flux and composition) throughout Solar System history (e.g. Spudis 1996, Crawford 2004, NRC 2007). Some of these objectives are astrobiological in nature, in that they will enhance our understanding of the cosmic conditions under which life first arose on Earth (Crawford 2006). However, although the *Clementine* and *Lunar Prospector* missions have in recent years greatly added to our knowledge of the geochemical and mineralogical makeup of the Lunar surface, our knowledge of the interior still largely relies on geophysical measurements made during the Apollo programme. As can be seen from Figure 1.1, these landing sites are all located at low to mid-latitudes close to the centre of the Lunar nearside, and were thus unable to provide anything approaching global coverage. In order to build on the Apollo data, and thus advance our knowledge of Lunar science, the *LunarEX* mission will fly 4+ penetrators to the Moon for the purpose of conducting a range of *in situ* geophysical and geochemical measurements at widely separated localities.

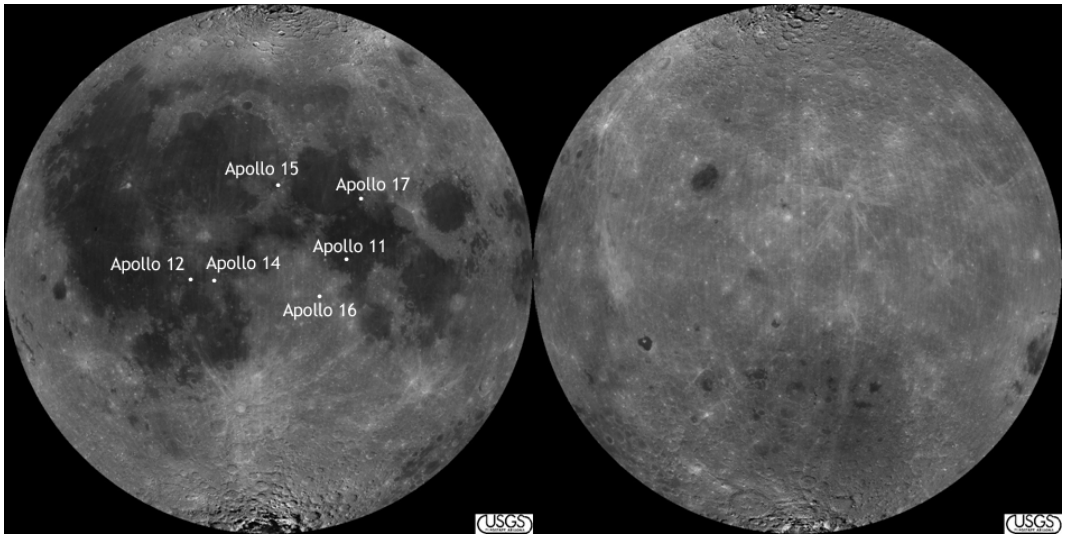

Fig. 1.1. Locations of the Apollo landing sites on the nearside of the Moon (left); the farside is at right. *The Apollo seismic network occupied an approximate equilateral triangle, roughly 1200 km on a side, defined by the Apollo 15 site at the northern apex, Apollos 12 and 14 (close together at the SW apex), and Apollo 16 at the SE apex. The two Apollo heat-flow measurements were made at the Apollo 15 and 17 sites. No long-term geophysical measurements were made at the Apollo 11 site. Note the geographically restricted nature of these measurements.*

1.2 Penetrators

Penetrators allow key scientific investigations of airless solar system bodies via affordable pre-cursor missions. In fact, it is difficult to envisage any other method which allows globally spaced surface exploration of airless planetary bodies that is not prohibitively expensive.

(Kinetic) Penetrators are small probes which impact planetary bodies at high speed and bury themselves into the planetary surface. For the Moon we propose deployment of ~13Kg penetrators that are designed to survive impact at high speed (~ 300 m/s) and penetrate ~2-5m. The impact process generates decelerations of up to 10,000g, which together with the low mass, restricts the type and capability of payload that can be accommodated. However, a

surprisingly large range of instruments have already been constructed and qualified for penetrator use, and an ever widening range of scientific instruments have a robust nature which lend themselves to the necessary ruggedisation. Of course, multiple penetrators allow a natural level of redundancy.

Survival at these impact speeds has been demonstrated by ground tests of NASA DS2 and Japanese Lunar-A probes, and extensive military experience of impacts into materials mostly consisting of sand, concrete, steel and ice.

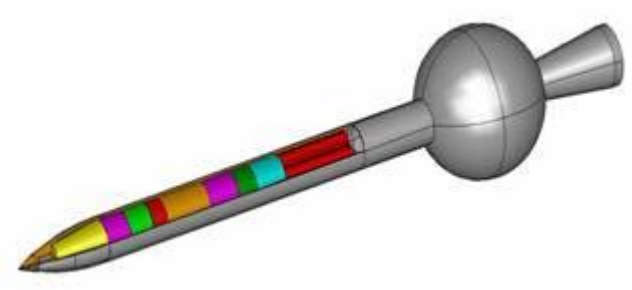

Figure 1.2 – Penetrator schematic

1.3 Current and Future Space Missions

Though there are several orbiter space missions with near term launch dates expected in the 2007-2008 timeframe (the Indian Chandrayaan-1, Chinese Chang'e 1, and the Japanese Selene), none of these will be able to address the main science issues we propose that require a seismic network, or provide in-situ ground truth investigation of water/volatile deposits in the sub-surface Lunar polar regolith. The Lunar Prospector impact produced no useful data about the Moon's composition. The NASA LRO (Lunar Reconnaissance Orbiter) mission includes an impactor (LCROSS) with a flyby investigation of the resulting material thrown high up above the Lunar surface. This could be capable of detecting water, and with an expected launch date of 2008 these results should soon become known. The deployment of multiple penetrators with LunarEX could provide ground truth corroboration, and multi-site quantitative characterisation of any LRO and other mission results.

LunarEX is based on the MoonLITE mission concept (Gao et al 2007) which is presently under funding review within the UK, but with LunarEX having a more sophisticated payload. While there is clearly an international interest in Lunar penetrator missions, LunarEX could be the first to be realised, (Lunar-A has been cancelled, after many years of study Luna-Glob remains in an assessment phase, and the future of MoonLITE is uncertain).

In summary, LunarEX has the potential to provide exciting Lunar science; provide information about the existence, concentration and form of any water ice deposits important for future Lunar manned exploration; provide a confidence building technical demonstration of penetrator technology applicable to cost effective pre-cursor in-situ exploration of other solar system bodies; and enable development of a technical capability with consequent benefits to European industry.

2. Scientific Objectives

The top-level science objectives for *LunarEX* fall into four categories: seismology, heat-flow, geochemical analysis, and polar volatile detection. We now address these four objectives in more detail.

2.1 Lunar seismology

Seismology is the most powerful geophysical tool available to us for determining the interior structure of a planetary body. However, to-date the only object, other than the Earth, where it has been applied with some success is the Moon, where the Apollo missions deployed a network of four highly sensitive seismometers close to the centre of the nearside. The Apollo seismometers remained active for up to eight years during which they provided important information on the Moon's natural seismic activity, and the structure of the Lunar crust and upper mantle (see Goins et al. 1981 and Lognonné 2005 for reviews). However, the deep interior of the Moon was only very loosely constrained by the Apollo seismology – even the existence, let alone the physical state and composition, of a Lunar core remains uncertain.

The main problem was that the Apollo seismometers were deployed in a geographically limited triangular network (between Apollos 12/14, 15 and 16; Fig. 2.1) on the nearside. As a consequence, the information obtained on crustal thickness and upper mantle structure strictly only refers to the central nearside and may not be globally representative. Moreover, seismic waves capable of probing the deep interior had to originate close to the centre of the farside, and were therefore limited to rare, relatively strong, events. Indeed, the tentative seismic evidence for a Lunar core arises from the analysis of just one farside meteorite impact that was sufficiently strong to be detected by more than one nearside Apollo seismic station in eight years of operation. This is clearly an unsatisfactory state of affairs, and there is a pressing need for a much more widely-spaced network of Lunar seismic stations, including stations at high latitudes and on the farside. Penetrators delivered from orbit are ideally suited as a means of emplacing a global seismometer network, which would address the following scientific issues:

2.1.1 Size and physical state of Lunar core

As the Apollo seismic data were unable to constrain the size or physical state of the Lunar core, such knowledge as we have has been obtained from studies of the Moon's moment of inertia, physical librations (as determined by laser reflector measurements), and electromagnetic induction studies (see Wieczorek et al. 2006 for a review). These studies favour a small ($R<400$ km) partially liquid core, with suggested compositions ranging from iron-nickel, Fe-FeS alloy, or molten silicates. Whether this liquid 'core' possesses a solid inner core is currently unknown. Information on the size, composition and physical state of a Lunar core would have profound impacts on our understanding of the Moon's origin, mantle evolution, and magnetic history. The latter point, when combined with studies of remnant magnetisation of surface rocks, will have important implications for our understanding of the origin and evolution of planetary magnetic fields. For these reasons, constraining the nature (and even the existence) of a Lunar core is the top scientific priority of the penetrator-deployed seismic network.

2.1.2 Deep structure of the Lunar mantle

One of the main contributions that Lunar science can make to planetary science more generally is an enhanced understanding of the internal differentiation processes that occur immediately after the accretion of a terrestrial planet. Magma oceans are likely to have been a common phase in the early evolution of all rocky planets, and, in contrast to the more evolved mantles of the larger terrestrial planets, the structure of the Lunar mantle may preserve a record of these early times. Seismology may help elucidate these processes in several ways.

Most fundamentally, seismology may be able to determine the initial depth of the magma ocean, and thus the fraction of the Moon's volume that was initially molten. The Apollo data appear to indicate a seismic discontinuity at a depth of about 550 km, which is sometimes interpreted as the base of the magma ocean (see review by Wieczorek et al. 2006). However, because of the placement of the Apollo seismometers, it is not currently known whether this discontinuity is global in extent or exists only under the nearside. A competing explanation is

that it represents the depth to which later partial melting has occurred which led to the formation of the nearside mare basalts. As noted by Wieczorek et al. (2006), distinguishing between these two possibilities is of key importance in understanding Lunar mantle evolution.

In addition, measurements of seismic wave speed as a function of depth help constrain the mineralogy of the mantle (e.g. Lognonné et al., 2003). This in turn may be used to constrain both the bulk composition of the Moon (and thus its origin), and the crystallisation history of the Lunar mantle and its implications for magma ocean evolution. Again, new, and more widely spaced, seismic data are now required if new advances are to be made over what has been learned from the Apollo data.

2.1.3 Thickness of the farside Lunar crust

Reinterpretations of the Apollo seismic data have now constrained the thickness of the nearside anorthositic crust to about 30-40 km (Khan et al. 2002, Lognonné et al. 2003, Wieczorek et al. 2006). However, the thickness of the farside crust has not been constrained seismically at all. Estimates based on gravity data are typically in the range 70-90 km (Wieczorek et al. 2006), but these are non-unique, and in particular depend on whether the Lunar highland crust should be considered as a single anorthositic layer, or as two layers with the lower layer having a more mafic (Fe-rich) composition. Farside measurements are required in order to determine the average Lunar crustal thickness which, because of its very aluminium-rich nature, has significant implications for understanding the bulk composition (and thus origin) of the Moon.

In addition, there is considerable interest in the thickness of the crust (if any) remaining under the giant South Pole-Aitken (SPA) impact basin on the farside – the largest impact structure currently known in the Solar System. Together with the nearside Procellarum KREEP Terrain (well studied by Apollo) and the farside highlands, the floor of the SPA forms one of the three main Lunar terrains identified by Jolliff et al. (2000). Part of the interest in the SPA lies in the possibility that it may have exposed lower crustal or upper mantle materials. Seismometers located within the SPA will, for the first time, be able to make a definitive measurement of the crustal thickness remaining under this important structure.

2.1.4 Studies of natural Moonquakes

The Apollo seismometers detected four types of natural Moonquake: (i) deep (700-1200 km), relatively weak, Moonquakes which occur in ‘nests’ and which appear to have a tidal origin; (ii) shallow (5-200 km), relatively strong, Moonquakes of unknown origin; (iii) thermal Moonquakes due to thermal stresses in the near surface; and (iv) meteorite impacts (summarised by Vaniman et al. 1991). Of these (i), (ii) and (iv) may be used as sources of seismic energy to probe the Lunar interior, and a better understanding of the causes and clustering of (i) will provide additional knowledge of the physical properties of the deep Lunar interior.

However, it is the shallow Moonquakes (ii) that are probably the most interesting scientifically. These were the strongest (up to magnitude 5) and rarest (only 28 recorded in 8 years), and currently their cause is unknown. Insofar as these result from unknown tectonic processes, our knowledge of present-day Lunar geological activity will remain incomplete until their cause and locations can be identified (e.g. Nakamura 1979). Owing to the spatially restricted locations of the Apollo seismic stations, the Apollo data lacks the resolution to pinpoint the precise epicentres or depths of these events, for which a global distribution of seismometers will be required.

Understanding these events is also important in the context of future Lunar exploration. For example, a magnitude 4-5 Moonquake is sufficiently strong that it would be prudent not to construct a Lunar base at localities where they are likely to occur (Neal 2005). Some

scenarios for future Lunar exploration also envisage placing optical astronomical instruments on the Lunar surface, and knowledge of Lunar seismicity could be useful in deciding where to site such instruments. Thus, in addition to providing fundamental information about Lunar geophysics, a better understanding of the origins and locations of shallow Moonquakes would make a significant contribution to future Lunar exploration.

2.2 Lunar heat-flow

Measurements of surface heat-flow provide valuable constraints on the composition and thermal evolution of planetary interiors. To date, the only planetary body other than the Earth for which surface heat-flow has been measured *in situ* is the Moon, during the Apollo 15 and 17 missions (Langseth et al. 1976). However, both these measurements were relatively close together on the nearside (Fig. 2.1) and may thus not be representative of the Lunar heat-flow as a whole. Moreover, both these Apollo measurements have been subject to numerous re-interpretations over the years, owing to uncertainties in determining the thermal conductivity of the regolith, the extent to which the temperature sensors were in contact with the regolith, and the uncertain effects of local topography (both measurements were very close to highland/mare boundaries).

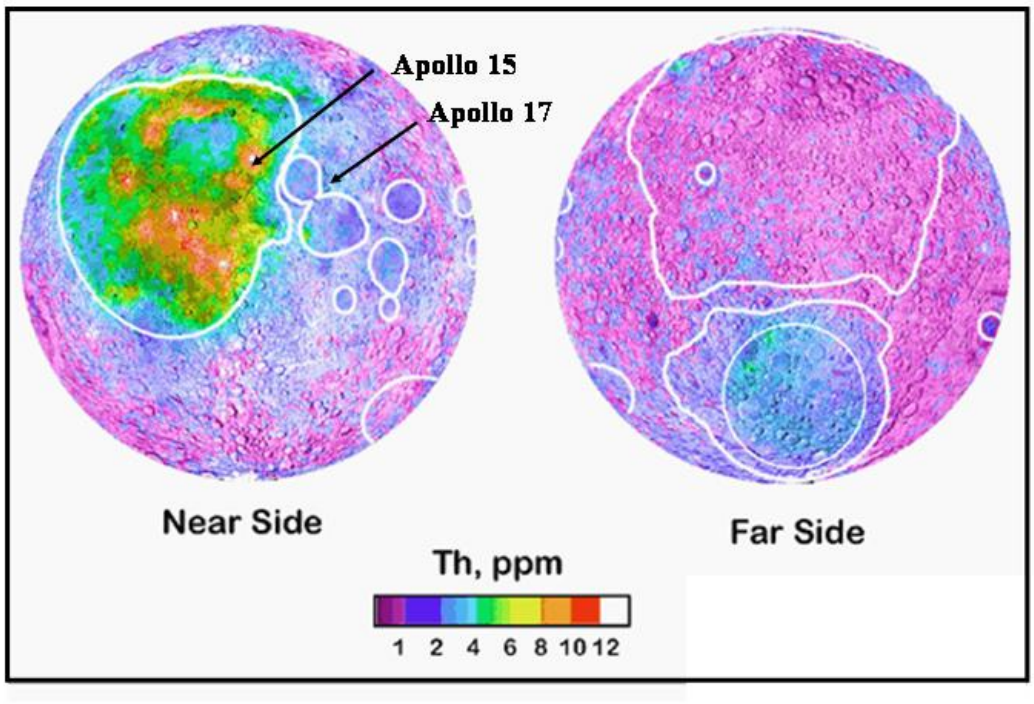

Fig. 2.1. Concentrations of Th in the Lunar surface, measured by the Lunar Prospector spacecraft. The PKT is the region of high Th concentrations around and to the south of the Imbrium basin on the nearside.

One particularly important measurement would be to determine the heat-flow as a function of distance from the Procellarum KREEP Terrain (PKT) on the north-western part of the Lunar nearside. Remote sensing measurements have determined that the heat-generating elements (U, Th, K) are concentrated at the surface in this area of the Moon (Fig. 2.1), but a question remains over whether this is a surficial effect (owing to excavation of a global underlying layer of incompatible element-rich material by the Imbrium impact), or whether these elements are indeed concentrated in the mantle below the PKT. The latter scenario would predict a much higher heat-flow in the PKT than elsewhere, and would have major

implications for our understanding of the early differentiation and crystallization of the Moon (e.g. Wieczorek and Phillips 2000). While the Apollo 15 and 17 data do appear to indicate a decrease in heat-flow away from the PKT (21±3 and 16±2 mW/m^2, respectively; Langseth et al. 1976), the experimental uncertainties are such that it is far from clear that this trend is statistically significant. In addition, Hagermann and Tanaka (2006) have drawn attention to fact that the Apollo results may simply reflect the different thicknesses of (U, Th, K-rich) Imbrium ejecta at the two Apollo sites, and not the underlying mantle heat-flow.

For all these reasons there is a pressing need to extend these measurements to new localities far from the Apollo landing sites (e.g. the polar regions and the farside highlands). Such measurements would greatly aid in constraining models of Lunar thermal evolution. Finally, we note that *in situ* measurements of both the temperature and the thermal conductivity of the regolith in permanently shadowed polar regions (which would be inherent in any heat-flow measurement) would be valuable in constraining the possibilities for frozen volatiles, which are another of our key scientific objectives (see below). Penetrator deployment of a global heat-flow network would be an attractive means of achieving these objectives.

2.3 In situ geochemistry

The only places on the Moon from which samples have been collected *in situ* are the six Apollo landing sites (Fig. 1.1) and the three Russian Luna sample return missions from near the Crisium basin on the eastern limb of the nearside. No samples have been returned from the polar regions or the farside, greatly limiting our knowledge of Lunar geological processes. Although, statistically, many of the 50+ Lunar meteorites must be derived from these unsampled regions, the provenance, and thus geological context, of any given meteorite is unknown, which limits their value in interpreting Lunar geology.

Although sample return missions to a number of currently unsampled regions would be the preferred means of furthering our knowledge of Lunar geological diversity, this may not be practical in the short term. An alternative would be to make *in situ* geochemical measurements, at least of the abundances of the major rock-forming elements (e.g. Mg, Al, Si, Ca, Fe and Ti). In principle this could be achieved by X-ray fluorescence spectroscopy, using instruments similar to the X-ray Spectrometer (XRS) designed for Beagle2 (Sims et al. 1999). Penetrator-deployed XRS devices therefore have the potential to determine the composition of Lunar materials in regions remote from areas sampled to-date. In addition to providing a great deal of information about the geology of the particular sites visited, such measurements would provide additional ‘ground truth’ for the calibration of remote-sensing instruments on forthcoming Lunar orbital missions (e.g. Chandrayaan-1, SELENE, and LRO).

2.4 Polar volatiles

As is well known, the *Lunar Prospector* neutron spectrometer found evidence for enhanced concentrations of hydrogen at the Lunar poles, which has been widely interpreted as indicating the presence of water ice in the floors of permanently shadowed polar craters (Feldman *et al*. 1998). This potentially very important result is still awaiting confirmation, but if water ice is present it is most likely derived from the impacts of comets with the Lunar surface (although solar wind implantation and endogenic sources might also contribute). The confirmation of water ice (and other volatiles) would be important for at least three reasons:

(i) Even though the original cometary volatiles will have been considerably reworked by impact vaporisation, migration to the poles, and subsequent condensation, it remains possible that some information concerning the composition of the original sources will remain. Among other things, this may yield astrobiologically important knowledge on the role of comets in 'seeding' the terrestrial planets with volatiles and pre-biotic organic materials (e.g. Chyba & Sagan 1992, Pierazzo & Chyba 1999).

(ii) As pointed out by Lucey (2000), Lunar polar ice deposits may be of considerable astrobiological interest even if they do not preserve any vestigial information concerning their cometary sources. This is because any such ices will have been continuously subject to irradiation by galactic cosmic rays and, as such, may be expected to undergo 'Urey-Miller-like' organic synthesis reactions. Analogous reactions may be important for producing organic molecules in the icy mantles of interstellar dust grains, and on the surfaces of outer Solar System satellites and comets, but the Lunar poles are much more accessible than any of these other locations.

(iii) The presence of water ice at the Lunar poles would be a very valuable resource in the context of future human exploration of the Moon (as a potential source of oxygen, rocket fuel and drinking water). Confirmation of its presence would therefore make a significant contribution to the developing Global Exploration Strategy which has renewed human exploration of the Moon as a key element.

We consider that volatile detectors, deployed on penetrators and landed within permanently shadowed craters, would be a powerful and economical means of determining whether or not scientifically and operationally valuable deposits of volatiles exist at the Lunar poles.

2.5 Conclusion

By deploying a range of instruments (e.g. seismometers, heat-flow probes, X-ray spectrometers and volatile detectors) to diverse locations on the Moon from which geochemical and geophysical measurements have not yet been obtained (including the poles and the farside), the LunarEX penetrators have the potential to make major contributions to Lunar science. At the same time, they will provide knowledge (e.g. of Lunar seismicity and polar volatile concentrations) that will be of central importance in the planning of future human missions to the Moon, and will also demonstrate a technology that will have wide applications for the scientific investigation of airless bodies throughout the Solar System.

3. Mission Profile

One Lunar **orbiter** spacecraft is required, which carries all the descent modules (4+). Each **descent module** is deployed from the spacecraft and comprises a **de-orbit motor**, **attitude control system** and **penetrator**, in-essence a micro-spacecraft in its own right. Just prior to impact the descent module motor and attitude control system are ejected from the penetrator. Penetrator releases will occur over a period of ~2 months. During descent communications from the descent module (including housekeeping and descent camera images) will be made via the orbiter using the penetrator's communication system. When line-of-site contact between descent module and orbiter is lost, information will be stored within the penetrator for later transmission. During surface operations the orbiter will relay the penetrator information to the Earth.

Key Mission parameters are shown in Table 3.1.

Table 3.1 Key Mission Parameters

Mission Duration	1 year.
Orbiter height	100km.
Orbit inclination	~90^{o}
Mean data rate	30 kbits/day
Number of penetrators	4 (with an option to increase to up to 8)
Penetrator location	Widely spaced, including: shaded pole (e.g. Shackleton), far side, and PKT (e.g. near Apollo 12 site).

3.1 Launcher requirements

The nominal mass budget of 846 Kg for a nominal 4 penetrators shown in Table 5.1 is compatible with a Soyuz-Fregat launch with ~30% free capacity.

3.2 Orbit requirements

The orbiter is required to operate in a 100 km polar Lunar orbit to deploy the penetrators in sequence for impact into the Lunar surface near the poles, the nearside and farside. Surface operation across the Lunar globe requires the orbiter to act as a communication relay after penetrator deployment.

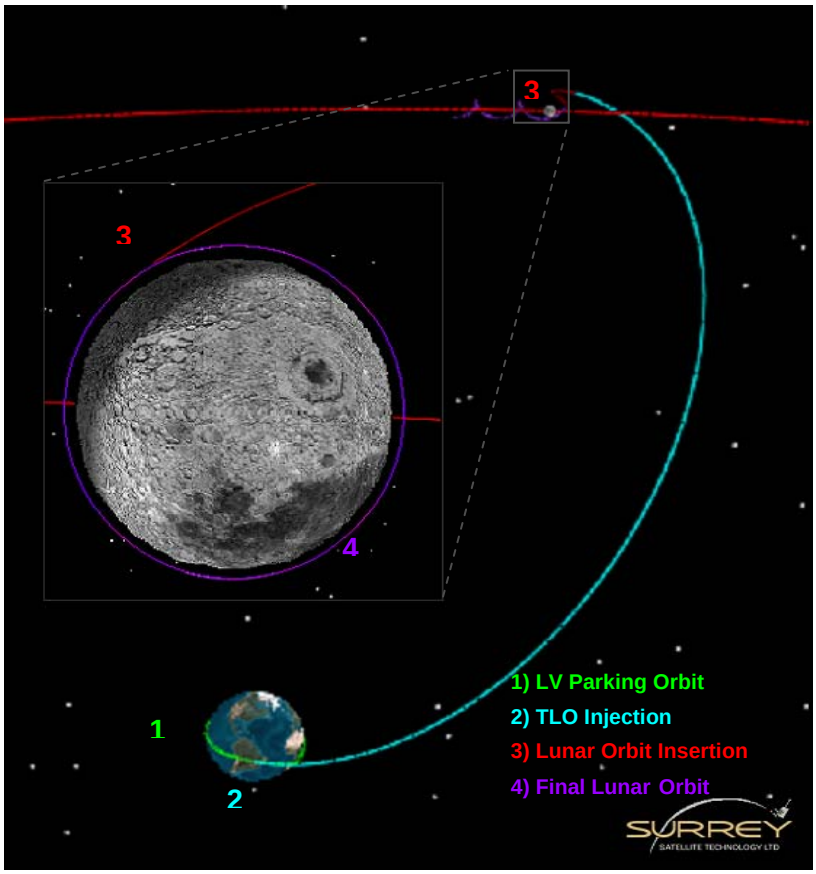

Figure 3.1 Earth to Moon transfer

Using the MoonLITE mission design as a baseline (Gao et al 2007), the spacecraft takes a direct transfer trajectory to the final Lunar orbit as illustrated in figure 3.1, which combines a low ΔV (reduced propulsion system costs), short Earth-Spacecraft distances (simpler communications system) and short transfer times (lower operations cost during transfer). This transfer takes approximately 3 days. The descent strategy of the penetrator and associated trajectory are as follows (see figure 3.2):

1. Carrier spacecraft first enters a 100 x 40 km altitude elliptic orbit.
2. Penetrator is released at periapsis.
3. Penetrator performs deceleration burn of approximately 1675 m/s to cancel orbital velocity.
4. Approximate 3.5 minute free fall to surface
5. Surface impact
6. Orbiter moves to final orbit and provides communications rely for penetrator to Earth.

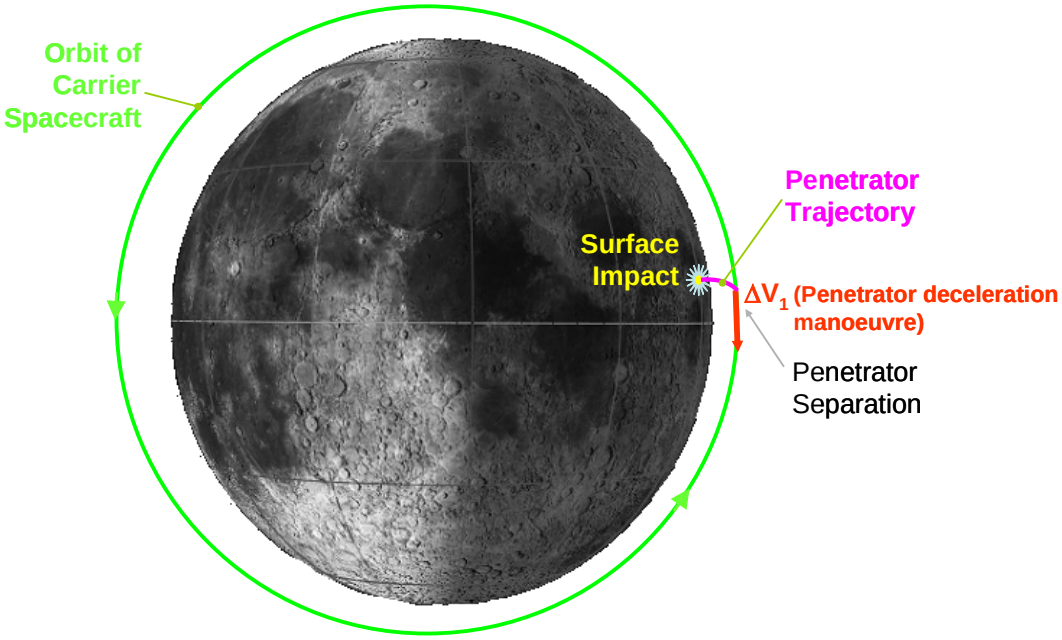

Figure 3.2: Penetrator descent trajectory

3.2.1 Penetrator Impact Error Ellipse

A knowledge of the error ellipse is essential when selecting impact sites. When calculating the size of the error ellipse a number of sources of error must be considered relating to the complex sequence of propulsive manoeuvres required to de-orbit the penetrator. The most important factors affecting landing accuracy are as follows:

- Magnitude of deceleration delta-V
- Direction of deceleration delta-V
- Accuracy of orbit of carrier spacecraft prior to penetrator release
- Orbit accuracy of the carrier spacecraft.

These errors were individually applied to the nominal penetrator descent to investigate their effect on the point of surface impact.

The error ellipse was estimated using the following error values: ±2% error in delta-V magnitude; and a delta-V alignment error in azimuth and inclination of ±2° (Assumes VNC reference frame for error analysis). In addition, a timing error (position of deceleration burn around orbit) was also considered. The results show that the main errors come from delta-V magnitude and azimuth. Of these, the magnitude error of the deceleration delta-V is likely to be significantly smaller than the ±2% shown (a typical value quoted by a supplier is only ±0.16%). Therefore, the major error results from the alignment of the thrust vector of the main burn. With a 2° error, a landing ellipse of 28km diameter is achieved. This conservative estimate can be compared with crater-targets at the Lunar poles. Shackleton (diam ~20km) would require only a modest increase in precision while Mawson (diam ~51km) provides an excellent alternative target. For non-crater targets the landing precision is more than adequate.

3.3 Ground segment requirements

Two ground stations would be suitable for LunarEX: E.g. :-

SSTL (RAL Antenna): Lat: 51.5°; Long: -1.3°
South Point (Hawaii): Lat: 19.0°; Long: -155.7°

The ground stations will be required to provide commanding for Orbiter orbit and attitude changes, descent module release operations (nominally 4 per mission, one every e.g. 2 weeks), and any non-nominal commanding. They will also be required for downlink of orbiter health and safety data, and penetrator science data. The frequency of contacts would be quite low e.g. typically one contact every 3-4 days.

The ground stations will also be required to provide commands to the individual penetrators via the orbiter. Such commands are needed to optimise the operation and data return from the payload. An externally referenced time signal is needed for operation of the seismometers as part of a global network.

There is no ground communication requirements for direct communication with the penetrators.

4. Payload instruments

4.1 Overview

The mission involves the delivery of a minimum of four penetrators into the Lunar surface at widely dispersed location. The general characteristics of the penetrators are given in table 4.1. Each penetrator comprises a scientific payload and support subsystems (power, communications, data management, structure). During the descent phase a camera (Penetrator Descent Camera) is used to provide impact site location and context information.

Mass (at impact)	13kg
Impact deceleration	Up to 10,000 g.
Impact angle (between impact velocity vector and tangent to surface)	~90° (not critical)
Attack angle (between penetrator long axis and impact velocity vector)	~<8° (critical)
Penetration depth into regolith	2 to 5m.
Ambient penetrator operating temperature:	-20°C to -50°C. (50K to 100K in shaded polar craters)
Mean penetrator power (subsystems & payload)	60mW.
Mission duration	1.2 years (1 year on surface)

Table 4.1 – Penetrator characteristics

The penetrator scientific payload is described in table 4.2.

Payload instrument Sub-instrument	**Mass (g)**	**Integrated power usage over 1 year mission (W.hr)**	**Telemetry Allocation (over 1 year) (Mbits**
Accelerometer and Tilt-meter	66	0.002	0.1
Geochemistry package	260	12.0	0.1
Water/Volatile Experiment	750	4.1	2.0
Seismometer	300	501.0	6.0
Heat Flow	300	1.0	0.6
Total Penetrator	**1676**	**516.1**	**8.8**
Descent Camera	160	0.05	2.0

Table 4.2 Penetrator Science Payload Elements

Below each scientific payload element is considered separately. Note that the TRLs given in this section do not include ruggedization necessary to survive penetrator impact. This issue is covered in section 7.

In the following sections it can be taken that unless otherwise stated: no special conditions apply; calibration involves comprehensive ground calibration (and maintenance of a flight representative unit on the ground during the mission); observing modes are simple (on and off); there are no special pointing or alignment requirements.

4.2 Impact accelerometer and tilt-meter

The main goals of this experiment are:

1. To derive mechanical properties of the Lunar regolith vs. depth at each impact site. This is of interest for comparison with existing models of Lunar regolith, and to provide context for the geochemistry experiment.

2. To provide key information for the other experiments, by determining:
    a. the depth below the surface at which each penetrator comes to a rest. This is needed for full interpretation of the thermal data for the heat flow determination.
    b. the angle from the local vertical at which each penetrator is tilted. This is needed to determine the orientation of the seismometer axes and to help measure the vertical temperature gradient for the heat flow determination.

3. To provide a full dynamic history of each penetrator impact, for comparison with results from ground testing and simulations.

4.2.1 Description and key characteristics

The goals listed above require two types of sensor: accelerometers and tilt sensors (inclinometers).

Accelerometry: two sets of 3-axis accelerometers will need to be located inside the penetrator close to its axis of symmetry. One set shall be mounted close to the penetrator tip, the other close to the penetrator's rear (upper) end. This is to derive the complete motion history of the penetrator (position and orientation) and compensate for the mechanical response of the penetrator structure. The accelerometers will operate during the impact event, sampled rapidly enough to achieve sufficiently fine spatial resolution of the motion. Such measurements are routine in military applications.

A resource / benefit trade-off will be required to select between 3 possible sensor configuration options:

- 2×3-axis orthogonal configuration, aligned with penetrator axes
- 2×3-axis orthogonal configuration, with symmetric alignment
- 2×3-axis orthogonal configuration, with symmetric alignment plus axial sensors

Tilt: a two-axis tilt measurement needs to be made to an absolute precision of 0.1° or better. This is driven by the need to correct the measured temperature gradient for non-vertical orientation of the penetrator and to properly interpret seismic data.

In addition, each sensor will require front-end analogue electronics (filter / amplification), analogue-to-digital conversion and interface to the common DPU and mass memory.

4.2.2 Performance assessment with respect to science objectives

Precise determination of the penetrator motion and final depth requires each of the accelerometers to have range, sensitivity, noise, offset performance and frequency characteristics that are compatible with the impact event. The sampling rate should be high enough to achieve sufficiently fine spatial resolution at the speed of impact. For 3 mm spatial resolution at an impact speed of 300 m s^{-1}, a sampling rate of 100 kHz is required.

4.2.3 Resources: mass, volume, power, OBDH and telemetry

	Accelerometry	**Tilt**
Mass [g]	56 for 8 sensors	10 for 2 axes
Volume [cm^3]	~1 per sensor, total ~8	25
Power [mW]	<500 for a short period only (10s)	<100 during measurements see below
OBDH	100 kHz sampling (equivalent to 3mm spatial) with 12-bit resolution for 8 axes, into 0.1 s duration circular buffer, frozen on impact. Onboard processing to reduce data volume	1 Hz sampling with 12-bit resolution for each of 2 axes, for the first minute after impact, then a few times per Lunar day thereafter.
Telemetry	0.1 Mbit total	1 kbit total

Table 4.3. Resource summary for accelerometer and tilt-meter

4.2.4 Pointing and alignment requirements

The accelerometers and tilt sensors will be mounted internally, with axes aligned with those of the penetrator.

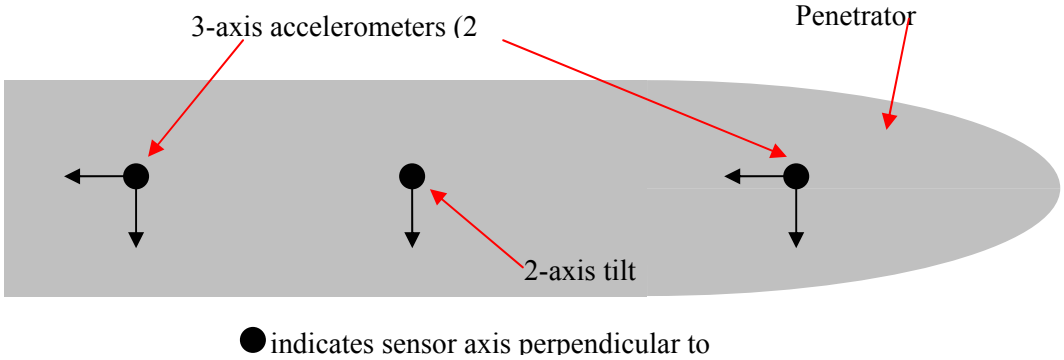

Figure 4.1. Schematic diagram indicating position and orientation of accelerometry and tilt axes inside the penetrator.

4.2.5 Current heritage and Technology Readiness Level

Accelerometry: TRL 8. COTS accelerometers available from companies including Endevco (e.g. model 7570A flown on DS-2), Kistler and Brüel & Kjær.

Tilt meters: TRL 6-8 depending on choice of sensor. Examples to evaluate for this application include:

- Incline sensors from the Taiko Device Group (Japan), which originate from automotive applications but were space qualified for use in the *Lunar-A* penetrators. For each axis a cylindrical cell is part-filled with a dielectric liquid and its level detected capacitatively by electrodes on the circular faces.
- Spectron L-series, as used by The Open University group on *Huygens* and the *Mars 96* penetrators

Fig. 4.2 Mars 96

- Analog Devices ADXL320
- Two-axis electrolytic inclinometer (e.g. from Fredericks Company)

Analogue front-end electronics: TRL 8 for the electronics themselves but TRL 6 for integrated system with high-g (potted) survivability (*Lunar-A* electronics: TRL 8).

Fast ADCs and solid-state data recorders: TRL 6 from military applications.

4.2.6 Proposed procurement approach & international partners

Procurement of COTS sensors for accelerometry. Procurement of COTS or modified COTS sensors for tilt. Integration and potting of electronics performed centrally for the whole penetrator payload. Experiment team expected to include relevant European penetrometry / accelerometry expertise from academia (currently at least 4 institutions) and industry.

4.3 Geochemistry Package

4.3.1 Description and key characteristics

The aim of the geochemistry element is to greatly improve our understanding of global Lunar geochemistry by performing in-situ analyses at globally dispersed sites, and to provide contextual information for related payload elements such as the Polar Volatiles detector and accelerometer. The requirement is therefore for one or more techniques that can detect and quantify the major rock-forming elements e.g. Mg, Al, Si, Ca, Fe, Ti.

The selected technique is X-ray spectrometry, for which the Beagle 2 X-ray Spectrometer (XRS) provides the benchmark. Primary excitation was provided by two ^{55}Fe (emitting X-rays of 5.90 and 6.49 keV) and two ^{109}Cd sources (emitting X-rays of 22.16 and 24.94 keV). Uniquely for an X-ray spectrometer, the sample was excited by two types of sources simultaneously as opposed to sequential source excitation used in some terrestrial X-ray Spectrometers (Potts et al., 1995) or single source excitation as with the APXS (Rieder et al., 1997). The fluorescent X-rays are detected by a Si PiN detector The instrument utilises excitation from radioisotope sources, identical to the Viking landers XRS, but uses the solid state detector as used by the APXS on Pathfinder. ^{55}Fe and ^{109}Cd sources provide excitation from primary X-rays of Mn (5.90 keV and 6.49 keV) and Ag (22.16 keV and 24.94 keV). The fluoresced X-rays are detected by a Si-PIN diode. The instrument is sensitive to X-rays in the 1-27 keV range and the corresponding range of detectable elements is from Na to Nb.

The baseline XRS is based on the Beagle 2 instrument and comprises two parts: the detector head assembly (DHA) and the Back End Electronics (BEE). The XRS will view the sample of the Lunar regolith brought into the penetrator volume by the micro-drill (see 4.4 below). Alternatively, a small x-ray transparent window with shutter could be provided in the rear wall of the penetrator.

4.3.2 Performance assessment

Expected accuracies and detection limits

Element	Si	K	Ca	Ti	Fe	Rb	Sr	Zr
XRS	-	0.11	0.070	0.098	0.034	0.10	0.15	0.047

Table 4.4a XRS Accuracy

Element	Si (µg/g)	K (µg/g)	Ca (µg/g)	Ti (µg/g)	Fe (µg/g)	Rb (µg/g)	Sr (µg/g)	Zr (µg/g)
XRS	-	360	230	120	420	13	14	9.0

Table 4.4b XRS Detection limits

4.3.3 Resources: mass, volume, power, OBDH and telemetry

	Geochemistry Package	
Mass [g]	Detector Head Assembly DHA: Back End Electronics BEE Shutter, window and mechanism* Total	60 100 100 260
Volume [cm^3]	DHA: BEE: Total	dia. 4.7 cm x height 4.7 cm 12.0 × 8.0 × 1.5 cm 160
Power [mW]	4000 for two periods of 3 hours each	
OBDH	No special requirement	
Telemetry	50 kb / spectrum, two spectra	

* shared with volatiles detector

Table 4.5 Geochemistry package resources

4.3.4 Current heritage and Technology Readiness Level

Heritage for penetrometer-borne XRS is provided by the ANGSTREM instrument in the aftbody of the Mars 96 penetrators. The LunarEX penetrator benefits from Beagle 2 heritage. Hence we assign TRL = 7 but must bear in mind that the instrument will require qualification at high-gee levels – see section 7.

4.3.5 Proposed procurement approach & international partners

Manufacture of XRS as a collaborative, international endeavour. Discussion with ANGSTREM team/descendents to learn lessons from Mars 96.

4.3.6 Critical issues

View of micro-drill sample volume vs window and shutter trade-study to be performed.

4.4 Water/Volatile detector

The measurement of volatile content in the shade, polar Lunar regolith is a key mission objective and so in order to provide unequivocal results, whilst ensuring redundancy in this key area, an integrated suite of complementary instruments is proposed. The analysis techniques and sample requirements are listed below:

Technique	**Method**	**Sampling requirements**
Mass spectrometry	Direct	Sample ingress / laser stand-off
Spectroscopic	Direct	Sample ingress
Mutual impedance spectroscopy	Inferred	Touch sensor
Pressure sensor	Inferred	Sample ingress
Calorimetric	Inferred	Sample ingress

Table 4.6 Water and Volatile detection techniques

Note also that *in situ* measurement of regolith electrical properties for interpretation of ground penetrating radar results from orbit.

4.4.1 Sample collection & Thermal control:

Sample collection is achieved with a micro-drill mechanism that is activated after impact. During operation the bit extends into the regolith and can deliver material tailings into a cup inside a sample collection container. Following the drilling operation, a pyrotechnic actuator

is used to seal the sample container preventing the unwanted escape of evolved gases during sample analysis.

A resistive heater is wound around the sample container to enable heating the collected regolith sample. The temperature of the sample during heating (and cooling) is measured by two sensors located inside the sample container. One sensor is attached to the wall of the container and the other is located on a thermally isolated post in the centre of the cup. Gases evolved from the sample during heating are vented through two capillary tubes to either the mass spectrometer or the optical analysis instrument.

4.4.2 Measurement techniques:

Mutual Impedance spectrometer: Laboratory studies of Lunar simulants have shown that a measurement of mineral dielectric constant is a suitable method of detecting water to levels of 0.1 % (with possible lower detection limits of 0.001%). The sensors are physically small, simple devices and so can be incorporated into the drilling mechanism allowing rapid in-situ measurements to be performed.

Calorimetric analyser: The sample heater will be programmed to deliver a stepwise heating profile to elevate the collected regolith materials to above the sublimation point of ice, hold it there for a pre-determined time before turning the heater off and the sample allowed to cool. During the heating-and-hold period, the recorded temperatures and power profile will reflect sample cooling i.e. when ice sublimates more energy is required to maintain the programmed heating ramp so the presence of ice can be detected in the power profile of the heating cycle.

Pressure sensor: As the stepped heating profile is conducted, evolved gases will expand into the analysis chamber and re-freeze when the heater power is switched off. The resulting pressure increase / decrease will be measured by a MEMS pressure sensor. The presence of water (and other volatile) ice will be detected in the temperature / pressure profile during sample heating and cooling.

Optical detection system: As the stepped heating extraction is conducted, evolved gases will expand into the analysis chamber. Spectroscopic analyses are conducted with a tuneable diode laser scanning across a single water line in the 1.37 μm region of the spectrum. The water vapour abundance in the chamber is calculated using Beer's law (*e.g. May et al., 1993*)

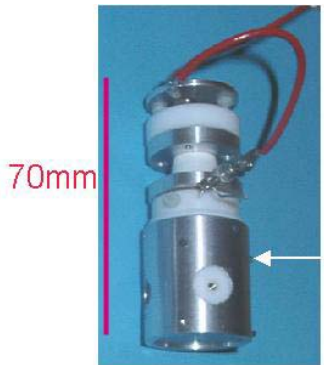

Mass spectrometer:

Characterisation and analysis of the evolved gases present in the sample chamber is performed by a miniature ion trap mass spectrometer. The measurement of the volatile composition together with the release temperature of individual volatiles is an effective tool for the identification and characterisation of the minerals and rocks found at the sampling site. A secondary mode of operation using a miniature laser as a stand-off laser ablation device would allow characterisation of regolith material through the wall of the penetrator, either in direct line-of-sight, or through a deployable fibre-optic cable.

Figure 4.3 Prototype, ruggedized ion trap mass spectrometer

4.4.3 Description and key characteristics

The integrated volatile detection experiment consists of a number of instruments and mechanisms. These are outlined below:

Sample collection and thermal control will consist of:

- A micro-drill mechanism to retrieve soil / regolith samples
- A sample container
- A pyrotechnic (one shot) seal
- Two miniature temperature sensors
- A resistively wound heater element (max temp 500^{o}C)
- A capillary leak to the mass spectrometer and optical detector

The drill is deployment-locked prior to operation. The first turns of the motor drill will release the locks.

Mutual impedance spectrometer:

- An impedance probe sensor is located on the outside of the penetrator
- An impedance probe sensor is on the drill bit, or a needle probe

Calorimetric analyser:

The technique uses the heaters and temperature sensors in the sample collection and thermal control system.

Pressure sensor:

- MEMS pressure sensor

Optical detection system:

- Miniature tuneable laser diode
- Thermal control system (heater and temperature sensor) for the laser
- Detector
- Capillary leak to sample chamber (via an isolation valve)

Mass spectrometer system:

- Miniature ion trap mass spectrometer analyser
- Field effect ion source
- Solid state detector
- Inlet capillary to sample chamber (via valve)
- Stand-off laser ablation

4.4.4 Performance assessment

A penetrator based water detection system utilising a sample drill, pyrotechnic seal, thermal control and spectroscopic detection system was space qualified for the NASA Deep Space2 mission.

Laboratory studies have shown that 0.1% water content can be detected in Lunar analogue material using the impedance spectroscopy technique.

The MEMS pressure sensor is a low mass, very rugged, fatigue-free, monocrystaline silicon diaphragm device, which has been qualified and flown on Beagle2 and Ptolemy (Rosetta Lander) instruments.

The ion trap mass spectrometer is an instrument based on that already developed for the Ptolemy instrument. Its small size, low mass and inherent ruggedness lends itself to location on a sub-surface penetrating device. Laboratory testing of a breadboard mass spectrometer system has demonstrated a mass range of 10 to 100 amu.

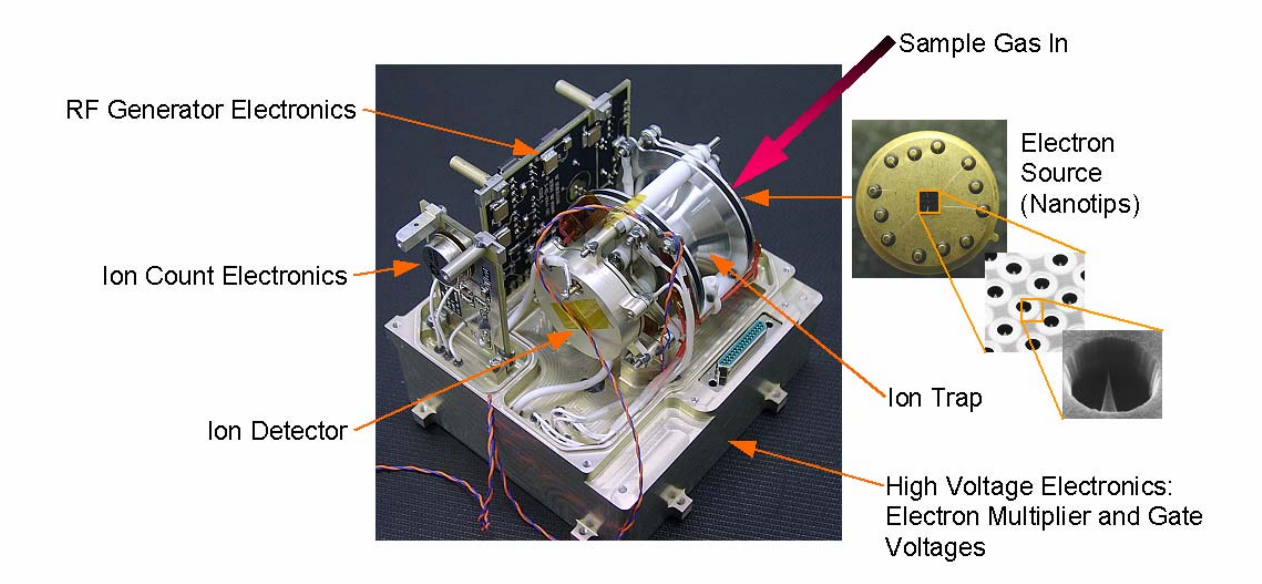

Figure 4.4 – Rosseta Ptolemy FM ion trap mass spectrometer which forms the basis of the proposed LunarEX mass spectrometer. Size approx 100x100x80mm; lid removed for clarity.

4.4.5 Resources: mass, volume, power, OBDH and telemetry

	Water/Volatile detector	
Mass [g]	Sample collection and thermal control	150
	Mutual impedance spectrometer	40
	Pressure sensor	10
	Optical detection system	50
	Mass spectrometer	200
	Electronics	300
	Total	750
Volume [cm^3]	1000	
Power [mW]	3000; duration 5000s in a number of stages	
OBDH	50 Mbits of data collected in a series of operations, on-board processing and compression required	
Telemetry	<2 Mbits	

Table 4.7 Water/Volatile package resources

4.4.6 Operating modes

A sequence of measurements is foreseen involving
Pre-impact checkout
Post-impact checkout
Sample collection (drilling)
Sample control (heating)
Water detection 1 (Mutual impedance spectrometer)
Water detection 2 (Heating / temperature)
Water detection 3 (pressure/optical)
Water detection 4 (mass spectrometer)

4.4.7 Current heritage and Technology Readiness Level (TRL)

Heritage for the sample collection and thermal control system is based on the drill and the pyrotechnic sample volume sealing device which flew on the NASA Deep Space 2 instrument (e.g. Smrekar et al., 1999). TRL 6/7

The pressure sensors are devices which are in use on the Ptolemy instrument on Philae the Rosetta Lander (e.g. Wright et al., 2007). TRL 8

The heritage for the optical detection system is based on the laser detection system which flew on the NASA Deep Space 2 instrument (e.g. Smrekar et al., 1999). TRL 6/7

The impedance spectrometer is based on proven mutual impedance probe which have been demonstrated on instruments flown on Philae the Rosetta (e.g. Trotignon et al., 2007 and Seidensticker et al., 2007) and Huygens (e.g. Fulchignoni et al., 2002) spacecraft. TRL 8. The subsurface element is based on mutual impedance probe being considered for mole deployment (e.g. Simoes et al.). TRL 4 and can be expected to increase as part of the HP3 instrument on ExoMars development.

The mass spectrometer is a compact version of the ion trap mass spectrometer system currently flying on the Ptolemy instrument on Philae the Rosetta Lander (e.g. Todd et al., 2007). TRL 4

4.4.8 Proposed procurement approach & international partners

Pressure sensors are COTS.
Optical detection system: COTS lasers and detectors available
Mass spectrometer: Lasers are being developed under ESA contract which may be applicable. FED sources COTS. Ion detectors COTS. Digital electronics either FPGA or ASIC development required.
Other items to be manufactured.

4.5 The microseismometer

4.5.1 Sensor description

The microseismometer elements are MEMS-based. A micromachined silicon suspension is used as the sensing element. This acts as a spring/proof-mass system, converting any external vibration to a displacement of the proof mass. This displacement is measured using a position transducer which consists of a series of electrodes on the proof mass and fixed frame forming a capacitive transducer together with sensitive readout electronics. The signal passes through a feedback controller and transconductance amplifiers to produce currents in a series of coils which form parallel electromagnetic actuators to maintain the position of the proof mass. There are two feedback loops, one producing the signal, and the second producing low-frequency integral control. One further coil is used to produce actuation from an external calibration signal. The design of the microseismometer indicating the sensor-head and electronics subsytems is shown schematically in fig. 4.5. These subsystems are described in more detail below.

The sensor head consists of a micromachined silicon suspension, incorporating the moving plates of the capacitance transducer and the feedback coils on the proof mass, sandwiching machined glass plates, one of which supports the fixed plates of the capacitance transducer, and a magnetic circuit which sits around the glass-silicon-glass sandwich. Along one side of the sensor head, which is 20mm square, accessed through a cavity in the upper glass plate, the electrical connections can be made to a series of metallised pads.

Fig. 4.6 shows the silicon suspension of the microseismometer fabricated at Imperial College, London. The suspension is formed by cutting through the 500µm thickness of a silicon wafer, using deep reactive-ion etching (DRIE). The clean profiles evident in the 30µm-wide flexures are the result of a concerted programme of DRIE optimization (Pike et al., 2004). In addition, the dynamics of the suspension are optimised to produce very good rejection of off-axis modes (Pike and Standley, 2005). The introduction of frames between the spring sets, and the mass relieving of these frames is evident in fig. 4.6.

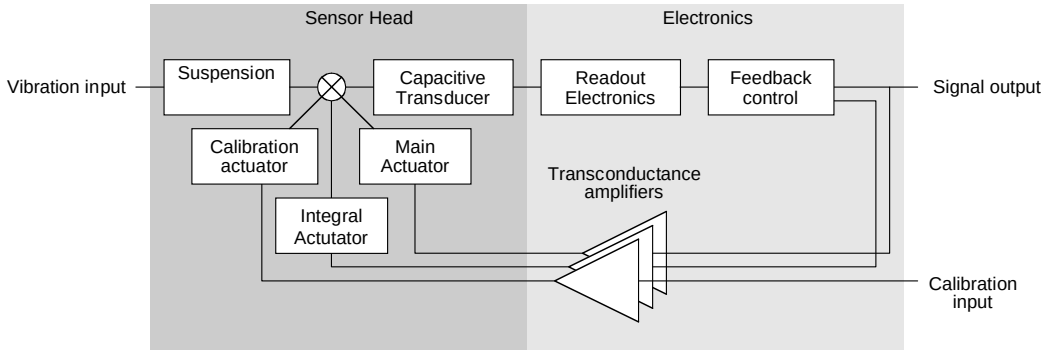

Figure 4.5. Schematic of the microseismometer

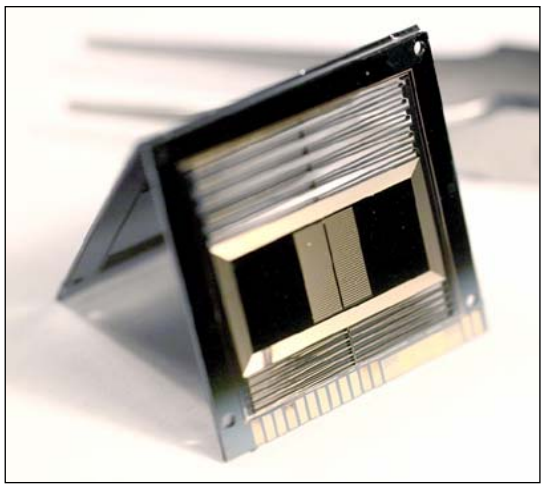

Figure 4.6. The silicon suspension of the microseismometer. The die is 20mm square.

The capacitance displacement transducer is of a novel design (Pike et al., 2006): the moving electrodes on the proof mass are in the form of an array which moves laterally over a similar array of fixed electrodes on the glass capping plate with the motion of the proof mass. Hence as the electrodes move in and out of registry with proof-mass motion, a periodic cycling of the capacitive coupling occurs. Optimisation of the design for this lateral capacitive array transducer, including the effects of stray capacitance, has been carefully studied and verified (Overmaat, 2005).

The glass plates on either side of the proof mass both seal and protect the suspension and, on one plate, carry the fixed electrodes of the capacitance transducer. In order to reduce damping and to allow for singulation of the plates from the original glass wafers, these plates are abrasively cut, from both sides. The silicon-glass sensor-head sandwich is bonded together to both seal the structure and provide the necessary interconnections to the capacitance electrodes.

Finally, a magnetic circuit is mounted either side of the sensor-head sandwich. This provides the magnetic field for the feedback actuator. This circuit has been designed, modeled by finite element analysis, and tested against the modeling to a better than 90% agreement. The circuit consists of four rare-earth, rectangular magnets, four pole pieces and two soft-iron yokes which close the circuit.

The electronics consist of a readout for the capacitance transducer, a feedback controller which splits the signal into in-band and low-frequency components, transconductance amplifiers to drive the coils, and pass-through for the calibration signal. This circuit is a variant on the electronics which have evolved over more than two decades under Kinemetrics for use in seismic sensors. As well as extensive verification of the performance of these electronics, Kinemetrics has detailed models which can be used to adapt the circuits for particular implementations.

4.5.2 Instrument Performance

The requirements for a seismic investigation of the Moon are based on data recorded during the Apollo programme.

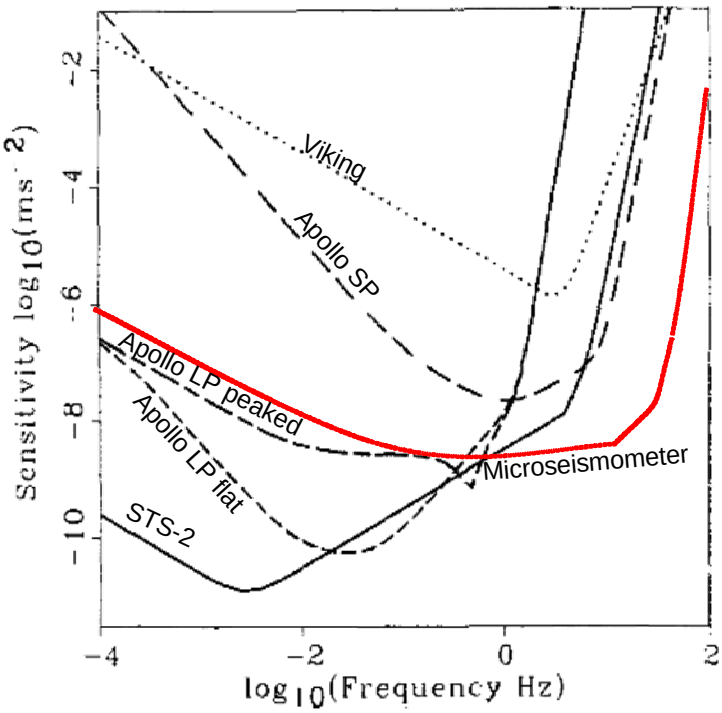

Fig. 4.7. Comparison of the microseismometer's performance to Apollo, Viking and terrestrial (STS-2) seismometers

Low-noise, high-sensitivity, well-coupled, isolated from ambient noise. All our science objectives require data with adequate signal to noise. The Apollo seismometers were able to acquire such data, and hence the microseismometer will match the performance of the Apollo instruments (Fig. 4.7).

Broad bandwidth**.** The majority of the LunarEX seismology objectives require observations of body-waves from moonquakes at regional and teleseismic distances. The microseismometer's bandwidth will be comparable to that of Apollo's

Three matched components**.** The identification of particular phases in body wave data is made more certain, and in difficult cases is only made possible, by using three-component data. A full three-component system is required, with matched horizontal components, in order to identify source direction, and to undertake more than qualitative waveform modelling and analysis. The determination of source depth, source extent, and anisotropy are all dependent upon full three-component data for their complete realisation.

Long operation time**.** To measuring a sufficient number of shallow Moonquakes to help elucidate their source requires a long duration. The mission lifetime of 1 year gives a reasonable expectation of sufficient Lunar seismic events to meet the LunarEX seismology science objective.

Parameter	Requirement
Noise	< 1ng/√(Hz)
Bandwidth	0.03 to 80 Hz
Temp. coefficient	100 ppm full scale/K
Nonlinearity	<1% full scale
Range	0.05 g

Table 4.8 Seismometer technical performance requirements

Linearity**.** Determination of scattering and attenuation properties, and waveform modelling for source depth, source extent, anisotropy, and core state, all require a linear instrument with a known amplitude and phase response. Analysis of surface waves has similar requirements.

4.5.3 Resources: mass, volume, power, OBDH and telemetry

	Microseismometers
Mass [g]	3 axes, each 100, total 300
Volume [cm^3]	200
Power [mW]	53 single axis, 112 full operations.
OBDH	10 samples per second / axis each 24 bit. Total data rate 720 bits/s. Data only transmitted when above a threshold, circular data buffer, 'event detection algorith'. Compression Higher rate sampling tbd for short periods
Telemetry	6 Mbits (corresponding to ~0.5% time during events)

Table 4.9 Seismometer resources

4.5.4 Pointing and Alignment Requirements

In order that the components of the Moonquake-induced vibration map sufficiently to the axes of the microseismometer, the vertical microseismosmeter axis, and hence deployment, should be aligned to better than 10 degrees to the Lunar surface normal. This requirement is only applicable during single, vertical-axis, operation. There is no absolute requirement on the azimuth, but knowledge of the azimuth will allow for complete vector determination of the vibration.

4.5.5 Operating Modes

Global network mode: 1-axis operation triggering 3-axis operation when a seismic event is detected.
Figure 4.8 shows typical Lunar seismic events from Apollo, notice that the time scale interval is 10 minutes. Note also the relatively larger signal seen in the horizontal axes compared with the vertical (z) axis. This is typical for the Moon but unlike the Earth where the vertical axis normally dominates. It is therefore proposed to use a horizontal axis trigger. The S-P travel times of the phases are typically more than 100s (Nakamura, 1983, Lognonne, 2003) which implies a requirement to initialize the other axes within that time – the microseismometers will have an initialization time of 30s.

Full operation mode: 3-axis operation
For local seismic events the time-lag between axes will be less and so it is proposed to operate a higher power mode in which all axes are continuously active. To conserve power this mode will operate for one month at the beginning of the mission in order to characterize the local

seismic environment. For the remaining mission the microseismometer will operate in a power-saving, 'global network mode'.

Sampling will be 10 24-bit sps with a bandwidth of 4 Hz, which covers most of the frequency range of moonquake energy. The baseline on-board data compression will be lossless and achieve an approximate three-times data volume reduction. For short periods a higher rate mode can be considered (200 24-bits samples per second)

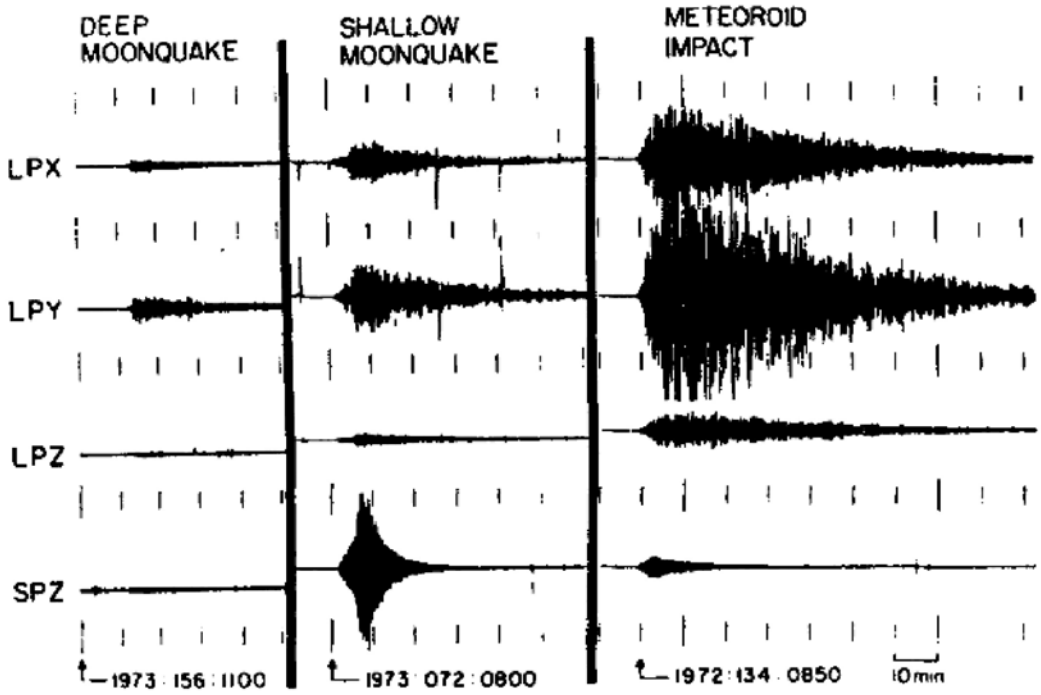

Figure 4.8 – Typical Apollo seismic events

4.5.6 Current Heritage and Technology Readiness Level

The microseismometer was originally developed for Netlander, a network geophysics mission for Mars, and is currently accepted and funded as part of the Geophysical and Environmental Package of ExoMars. Currently the microseismometer is at TRL 4 to 5, and the aim of the ExoMars programme is that all instruments will be at least 5.

4.5.7 Proposed procurement approach

It is proposed that the microseismometer and electronics are developed, fabricated and tested by Imperial and Oxford under research-grant funding.

4.6 Heat flow experiment

For measuring planetary heat flow, two parameters are required: the subsurface thermal gradient and the thermal conductivity of the subsurface material (i.e. the regolith). The heat flow experiment will measure the temperature gradient in the Lunar regolith by using temperature sensors on the outside of the penetrators. These will be accommodated at several locations between nose and tail. The thermal gradient can be determined from temperature measurements once the orientation of the penetrator is known from the tiltmeter. A correction will have to be made to deduct the thermal effect of the penetrator from the temperature measurements. The thermal conductivity of the subsurface regolith will be measured in four locations using small plate heaters. Thermal conductivity sensors could be measured using miniaturized needle probes.

4.6.1 Description and key characteristics

The heat flow experiment will consist of a number of sensors located on the outside of the penetrator. These are in detail:

- a suite of 8 relative temperature sensor (thermocouples) on the outside of the penetrator
- 4 absolute temperature sensors (Pt-100 or NTC thermistors) on the outside of the penetrator
- 4 miniature thermal conductivity sensors (e.g. heater plate with thermocouple, or miniaturized needle probe)

4.6.2 Performance assessment

The feasibility of a penetrator-based heat flow experiment has been studied in detail (e.g. Tanaka et al, 2000). Based on thermal sensors with an accuracy of 0.01K Tanaka et al. (1999) estimated an accuracy of 10% for the gradient measurement. Using plate heaters, thermal conductivity can also be measured with an accuracy of 10%. Needle probes increase this accuracy into the 1-2% range.

4.6.3 Resources: mass, volume, power, OBDH and telemetry

	Heat Flow
Mass [g]	12 temperature sensors: 120 4 thermal property sensors: 80 electronics: 100 Total 300
Volume [cm^3]	20
Power [mW]	25 normal ops 300 peak
OBDH	Temperature measurement: e.g. 1/hr., >18bit resolution, depending on chosen sensor. Thermal property measurement: 50Hz, 12bit resolution
Telemetry	< 0.5 Mbit for thermal property < 0.1Mbit for temperature

Table 4.10 Heat flow resources

4.6.4 Operating modes

Temperature sensors: temperature measurement
Thermal conductivity sensors: temperature measurement (low power) and thermal property measurement (high power).

4.6.5 Current heritage and Technology Readiness Level (TRL)

COTS space qualified NTC thermistors are available e.g. from Betatherm (http://www.betatherm.com)
Thermal sensors based on LUNAR-A flight heritage: TRL 8
The heat flow experiment on board the JAXA-ISAS LUNAR-A penetrators had flight readiness level.
Needle probe based on Mars-96: TRL 8
A needle probe for thermal measurement on board penetrators was developed for the Mars-96 penetrators.

4.6.6 Proposed procurement approach & international partners

Procurement of COTS thermistors or Pt 100, procurement of COTS thermocouples.

Manufacture or development of thermal conductivity sensors (depending on approach chosen)
International partners: Collaboration with JAXA-ISAS Division of Planetary Science anticipated.

4.7 Penetrator Descent Camera

4.7.1 Description and key characteristics

The Penetrator Descent Camera (PDC) does not have to withstand impact and so general space qualified camera technology will be suitable. For this the space qualified Beagle-2 PANCAM which are also in development for ExoMars are quite possible at quite low resource of 160g and 900mw, (Griffiths et al 2006), (these values are given as a baseline in table 4.2), though we propose a lower mass based on a 'camera on a single chip' 3 Mpixel CMOS detector coupled to a 45º objective lens (⅓" format) via minimal encapsulating structure. The PDC will image the surface in RGB colour from 40 km down to ~ 1 km altitude to determine landing site location and context; thus supporting the achievement of the science objectives. Below 1 km the image blur due to motion exceeds the camera resolution.

The camera would interface directly to the penetrator DHU transferring up to 32Mbit bits per image (binning operations of 2x2 and 3x3 to 1 pixel could be implemented in the DHU to conserve on board mass memory). Therefore, 4 images acquired during the 3 minute 42 second decent would require 30 Mbit of uncompressed storage. The storage requirements could be reduced by a factor of 15 by using lossy compression (e.g. wavelet).

4.7.2 Performance assessment

Expected PDC performance (based on a COTS mobile phone camera module) is shown in the following table.

Size (l x w x h) (mm)	10 x 10 x 30	Linear Resolution (m/pixel)	120 (@ 40 km) 3 (@ 1 km)
Array Size (w x h)	512 x 512	Pixel Size (µm)	2.2 x 2.2
Output Format (Bayer Matrix)	10 bit RGB	Angular Resolution (mrad/pixel)	0.3
Signal to Noise Ratio (dB)	42	Spatial Resolution (m at 1 Km)	0.3
Diagonal Field of View (º)	45	Drive Voltage (V)	2.8
Sensitivity $(DN/s)/(W/m^2.str.\mu m)$	168	Dynamic Range (dB)	50

Table 4.11 PDC Specifications

4.7.3 Resources: mass, volume, power, OBDH and telemetry

	Descent Camera
Mass [g]	10 (160 for Beagle-2 camera)
Volume [cm^3]	3
Power [mW]	160 during descent (~220s)
OBDH	'Offline' x10 data compression on 21 images (each 32 Mbits)
Telemetry	2 Mbits to be transmitted over 28 days, some transmitted during descent(tbd)

Table 4.12 Descent Camera resources

4.7.4 Pointing and alignment requirements

The optical axis to be within 1º of the penetrator axis

4.7.5 Calibration requirements

The PDC would be radiometrically calibrated to better than 1% and geometrically calibrated so that the relative alignment of the optical and penetrator long axis is known to better than 0.1º.

4.7.6 Current heritage and Technology Readiness Level (TRL)

Optical cameras for use in space are relatively common-place (certainly TRL>7) which could be employed here with modest use of resources, though we would aim to space qualify the lower mass and power COTS mobile phone camera modules for which the TRL is currently low at ~2. An international team of German, Swiss and Austrian collaborators would be assembled to develop the instrument (c.f. the Pan Cam consortium for ExoMars)

5. Basic spacecraft key factors

One Lunar **orbiter** spacecraft is required, which carries all the descent modules (4+). Each **descent module** consists of a single **penetrator** attached to a **de-orbit motor and attitude control system** which is ejected prior to impact.

5.1 Orbiter

The mass budget for the orbiter + descent modules is shown in Table 5.1. The Orbiter will include for each descent module - accommodation, commanding and telemetry communications (health status), power, and ejection mechanism.

Table 5.1 LunarEX Orbiter Mass Budget for nominal 4 penetrator payload (Gao et al 2007).

ITEM	**Mass (Kg)**
Structure	131.0
Communications	8.4
Power	28.7
Solar Panels	15.3
AOCS	44.1
Propulsion	66.1
OBDH	6.5
Environmental	16.6
Harness	30.0
Payload (4 descent modules)	158.4
System Margin (platform)	34.7
Total (Dry)	**539.7**
Propellant (Transfer, LOI, OM) AOCS Propellant	296.4 10
Propellant (Total)	**306.4**
Total (Launch)	**846.1**

5.1.1 Attitude and orbit control required

The AOCS system of the LunarEX spacecraft is required to perform 3-axis pointing for such tasks as orienting the spacecraft during the propulsive mission phases, antenna pointing for communications, directing solar panels towards the sun and launching penetrators towards the desired locations on the Lunar surface. After the deployment of the penetrators on the surface, the orbiter will continue to operate and communicate with the surface instruments and with Earth until the end of the mission. During this time ΔV orbit maintenance will be performed

to ensure adequate visibility with the surface instruments and the Earth ground station. The basic AOCS system requirements are summed up as below:

3-axis pointing accuracy:	1 degree
Array pointing accuracy (all phases):	5 degree
Lunar insertion pointing accuracy:	1 degree
Mission lifetime:	2 years

5.2 Descent Module

There will be four descent modules, each comprising of a penetrator and aft de-orbit and attitude control system which is ejected from the penetrator prior to penetrator impact. A descent camera will be mounted on the descent module. The overall mass of each descent module will be 39.6 Kg.

Upon release from the carrier spacecraft, the penetrator must perform a number of propulsive manoeuvres to safely reach the Lunar surface with the correct impact constraints. Typically an impact velocity not exceeding ~300 m/s and alignment of body axes no greater than 8° from the velocity vector (i.e. attack angle). The penetrator is released from the carrier spacecraft with a spin rate of typically 60 rpm to provide initial stability, and a period of typically 5 minutes is given to achieve a separation of 10m prior to starting the sequence. It is currently assumed that a spin-up and eject mechanism is used; however spin up of the carrier can be investigated as an alternative. The spin rate is limited to that needed for initial stability rather than that required to stabilize during the delta-V in order to keep the mechanism as simple as possible.

Following separation from the orbiter several manoeuvres are performed during the course of the descent. These are as follows:

1. Spin-up to ~500 rpm
2. Deceleration burn of approx. 1675 m/s
3. Spin-down to ~20 rpm
4. Spin axis precession

Propulsion for the penetrator is based on several technologies, selected for each propulsive stage of the descent. The deceleration burn will use a solid motor due to the short burn duration required to reach the required delta-V (to minimize gravity losses). However, several technologies were considered for the other phases. These are cold gas, mono-propellant (Hydrazine) and small solid rocket motors. The combinations of these technologies that were considered are as follows:

- All cold gas (too inefficient)
- Solid spin up/Mono-prop spin down/nutation/precession
- All mono-prop
- Solid spin up/down, mono-prop nutation damping/precession (mono too complex for small nutation damping only)

The selected baseline is to use a Solid Rocket Motor for the deceleration and a mono-prop (hydrazine) system for the remaining manoeuvres. This is primarily due to the mass/volume saving over a cold gas system and the simplicity of a single propulsion system for all phases (excluding deceleration burn) opposed to solid/mono-prop combinations. The motor developed for Lunar-A and available from Japan is one option.

Attitude Control of Penetrator with Effect to Attack Angle/Error Thereon

The attitude control system is required to stabilize the penetrator during the firing of the solid motor, and then reorient to the local nadir to an accuracy of approximately 8 degrees and maintain that to impact. The penetrator is very constrained in mass, power and cost, hence these objectives must be met with a minimum of low cost hardware.

The simplest option for stabilizing the penetrator during the ~10-second burn is to spin about the longitudinal axis. This penetrator is prolate and hence nutationally unstable. Any nutation will grow in the presence of energy dissipation, leading to a flat spin after a given period (minimum energy state). The presence of propellant on board is a prime means of energy dissipation, however the time constant of the nutation growth is expected to be significantly longer than the burn period. Active nutation damping will be required during the spin down period to prevent nutation growth, and may also be applied during spin up and the delta-V.

A fuller study of this issue is published in (Gao and Phipps, 2007).

5.3 Penetrator

Each penetrator will be ~0.5m long and ~13kg mass (similar to Lunar-A) and will be a simple "single-body" type (as opposed to fore-/aft-body types such as Deep Space-2). They will each consist of a supporting structure, a power system, comms system, data handling system, and payload.

A preliminary study of penetrator structure options has been carried out by QinetiQ (Church, 2007). Four alternative materials were considered, steel, aluminium alloy, titanium alloy and carbon composite. A summary of results from this study are shown in table 5.2.

Penetrator Shell Material (for 720mm length)	Wall Thickness (mm)	Projectile Internal Volume (l)	Projectile Filling Mass (kg)	Projectile All-up Mass (kg)
Aluminium Alloy	6.5	6.5	7.44	13.0
Steel	11.5	5.70	6.5	27.4
Titanium	2.5	7.36	8.46	10.8
CFRP Compression Moulding	7	6.4	7.33	10.5

Table 5.2 Penetrator Structure options

These figures should be compared with an estimated payload volume requirement of:

Scientific payload elements - 1.5 litres
Batteries - 1 litre
Electronics - 1.5 litre
Total - 5 litres

Occupancy factor - 50%

Total required volume - 10 litres

Therefore with Aluminium, Titanium and CFRP penetrator masses below the 13kg allocation are achievable. Indeed for Titanium and CFRP a further mass saving can be envisaged which would allow the inclusion of additional batteries. This lower mass c.f. Lunar-A arises largely from the significantly lower mass of the seismometer (~3kg on Lunar-A).

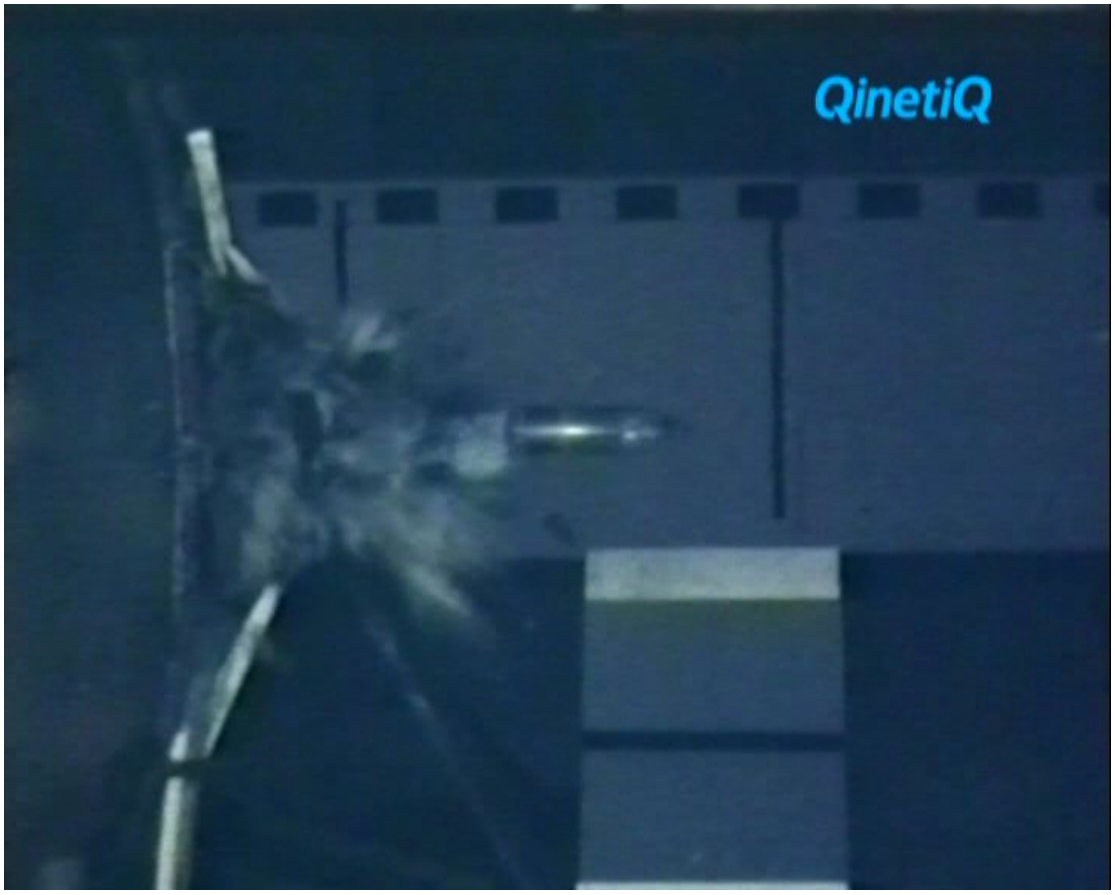

Figure 5.1 – Demonstration of a LunarEX sized 'penetrator' at QinetiQ Ltd. The impact velocity was ~300ms-1. The photo shows the item emerging after passing through 2m concrete – the final velocity was low and the impact was generally equivalent to LunarEX situation.

Given the level of expertise available from the defence sector and the results of the Mars-96, DS-2 and Lunar-A development programmes the TRL for the penetrator structure is estimated at level 5.

5.4 Subsystems, Heritage and Technical Readiness Levels

Other than the details of the ejection mechanism the overall concept of the Orbiter is not unlike a simplified Mars Express. All Orbiter subsystems have considerable heritage from previous missions.

5.4.1 Onboard data handling and telemetry

(a) Orbiter: Prior to penetrator deployment, the orbiter will need to provide commanding and power to each onboard descent module for a limited number of occasions to enable health checks. During deployment the orbiter will be required to accept descent module health checks, and if possible descent camera images. After deployment the orbiter will need to provide regular (e.g. every 15 days) communications with the penetrators for commanding and uplink of data, and to relay this information to Earth. The orbiter will also need to accept commands from Earth and telemeter to Earth a small amount of housekeeping data to support its own orbital manoeuvres and sub-systems.

(b) Penetrator: Because of the expected infrequent communication contacts with the orbiter, each penetrator will need to operate autonomously, collecting, compressing, and storing data until each uplink opportunity. A small commanding capability is necessary to allow

optimization of seismic data selection and data volume reduction. Because of the low radiation environment an FPGA, small micro-controller or micro-processor solution will be strong candidates for this mission with relatively high density memory. The nature of the scientific payload will naturally allow for a high degree of sequential operation with initial uplink of descent camera images and accelerometer data collected during impact. This will be followed by geochemical and temperature data. Heat flow measurements will not be possible until after thermal stabilization possibly after a whole Lunar cycle or more. Seismic data will be the only instrument required to operate more or less continuously throughout the whole mission. Thus, this will naturally allow, as resources permit, a significant processing and memory storage saving via natural prioritisation. In addition it will be planned to select only the most significant seismic data for transmission within the resources available.

5.4.2 Power

Because the penetrator will be completely buried under the Lunar regolith, and the sun is not visible in the permanently shaded craters, power will be entirely supplied to the penetrator systems by batteries. Initial studies for this proposal (Wells 2007) indicate the use of Lithium thionyl chloride primary cells, as planned or adopted for DS-2 and Lunar-A, with an energy density of ~275Wh/kg. The Lunar-A team report an energy density of 430Wh/kg (Mizutani et al 2005). For these batteries, both the operating temperature and g-force survival levels have significant margins over the LunarEX requirements. The initial study indicates a battery mass of the order of ~2.5Kg/penetrator, corresponding to a capacity of ~550W.hr (depending upon operating temperature). For non-shaded sites, operation of a penetrator comparable to Lunar-A dimensions should achieve a similar 1-year operational lifetime. For the shaded polar sites, where there are much lower temperatures, extended operations will require careful consideration of insulation and could greatly benefit from use of RHU's.

5.4.3 Communications

One contact/penetrator every 15 days, corresponds to a total of ~2W.hr for the necessary 90sec contacts (in a general 12 minute window). With a mean data rate of 30kbits/day this corresponds to an uplink rate to the orbiter of 5 kbits/s (5x Lunar A). A similar amount will be required for the receiver leading to around 4W.hr which is <1% of the total power budget, with ~99% of the power left for payload and data handling.

Following impact, each penetrator will be buried beneath the Lunar regolith, and the communications system adopted will be based on Lunar-A which relies on transmission through the regolith. However, a detailed study will be made of regolith communication transparency properties, and the possibility of a trailing antennae especially for the case of immersion into regolith containing a significant proportion of ice.

The baseline design is a body antenna mounted at the aft (trailing) end of the penetrator. The antenna would be conformed to the surface of the penetrator, to ensure a smooth, projection free surface. As the body diameter is quite small for a UHF antenna, a helical or similar antenna may be needed; alternatively dielectric loading could be employed at the expense of mass. The dielectric properties of the regolith would need to be taken into account in designing the antenna in order to optimise performance when buried. Testing would also need to replicate these conditions. The ruggedised UHF transceiver built by QinetiQ for the Beagle 2 mission to Mars, is proposed as a starting point. Its mass is approximately 600g, and its design is based on the highly successful MELACOM transponder, still in operation in Mars Orbit. MELACOM would be a logical unit to deploy on the Orbiter. The design could be updated and miniaturised for the LunarEX mission, with an emphasis on the engineering to survive the high gee environment. Study of the link budget shows that a 0.5W omni-directional UHF transmitter on the penetrator can transmit 15 days of data to the orbiter in ~90s with a more than adequate ~30dB of margin. The composition of the Lunar regolith will

have a significant impact on the achieved margin of the link for which a minimum margin of 20dB has been assumed to account for possible regolith attenuation on the link.

6. Science Operations and Archiving

It is assumed that the agency will be responsible for spacecraft operations support including telemetry, immediate health and safety monitoring, and any commanding that may be included. The scientific consortium will be responsible for detailed specification of agency operation requirements, more detailed health and safely analysis, calibration, scientific data analysis, and command generation.

6.1 Science Operations Architecture and share of responsibilities

Science operations for this mission are envisaged as follows :

(a) **Orbiting support spacecraft** – Intense operational support will be required for the launch, and early post launch phase, orbital manoeuvre changes, and then at a low level for regular spacecraft health and safety (housekeeping) monitoring throughout the nominal 1 year mission.

(b) **Penetrators** – It is envisaged that there will be intense operational support for pre-deployment health and safety checks, follow by orbital deployment, and impact. Deployment of penetrators will occur approximately every 2 weeks. Contact with each penetrator is expected every 15 days (more frequently for polar penetrators). After the initial 1-2 contacts only the seismometer and heat flow experiments will be operating, and operational support will be reduced.

Data collected during operations should be made available promptly to the science team for analysis.

In summary, operational support during the first 3 months will be relatively intense with a co-located science team assessing data and optimising the payload operations. For the latter part of the mission (following 9-12 months) operations will be relatively routine.

6.2 Archive approach

All scientific data should be archived. It is to be noted that the total penetrator data volume is expected to relatively small at ~30kbytes/day, generating 11Mbytes/yr * 4 penetrator mission = 44Mbytes for a complete 1 year mission.

6.3 Proprietary data policy

All the scientific data shall be made public 6 months after the end of the mission.
However, data of public interest from the descent cameras will be made publicly available immediately.

7. Key technology areas

7.1 Payload TRL level and technology development strategy

General Technology Readiness of payload instruments has been discussed in section 4 for each element. Here we discuss the suitability of each element to survive a peak impact acceleration level of 10,000g.

Accelerometer and Tilt-meter: Available off-the-shelf – no significant issue

Geochemistry package: Some heritage from Mars-96 ANGSTREM but further development required. Package inherently robust due to solid state nature of elements.

Water/Volatile Experiment: Mutual impedance spectrometer, heaters, sensors, pressure transducers, laser diode, mass spectrometer, electronics contain no moving parts and are therefore intrinsically rugged. The micro-drill concept has DS-2 heritage but will require further development for LunarEX

Seismometer: The MEMS based solution developed for ExoMars will require further development. A number of measures associated with clamping of the proof masses and alterations to damping constants through design have been examined and will require breadboard testing in the near term. These developments will be pursued in collaboration with, and build on, the expertise of the QinetiQ penetrometer group who have already hardened lower performance silicon sensors for use in projectiles.

Heat Flow: Intrinsically robust with significant heritage from Lunar-A and Mars-96, Philae and HP^3 project.

7.2 Mission and Spacecraft technology challenges

In many respects the mission is similar to other Planetary missions (e.g. Mars Express) albeit with a more local destination.

The key feature of the mission is the use of penetrators to deploy scientific instrumentation into the surface of a planetary body. This must be considered the principal challenge of the mission.

8. Preliminary programmatics/Costs

8.1.1 Overall proposed mission management structure

LunarEX is proposed as an ESA mission with international collaboration only occurring at the level of the payload

8.1.2 Mission schedule drivers

Within the UK there is a presently funded penetrator demonstration programme that is expected to demonstrate a proof of concept penetrator firing within 2.5 years. While the penetrator technology is relatively mature in the defence sector, and a great deal of experience has been gained with the Lunar-A and DS-2 projects, it can be expected that the main schedule driver will be the penetrator development.

Proposed milestones in penetrator development:

Proof of concept demonstration for LunarEX mission -	December 2009
Qualification of LunarEX Penetrator design -	December 2011
Earliest launch of LunarEX -	2013

The above schedule is consistent with that proposed for MoonLITE (as yet unfunded) which is targeting a launch in 2011-12, based on a more modest payload.

8.1.3 Payload/Instrument Costs

It is proposed that the penetrators themselves should be provided by ESA nations with non-ESA collaboration while the De-orbit motor and descent AOCS should be funded by ESA.

The following estimates assume 4 flight penetrators and 1 flight spare

ESA Payload Costs - 20 M€

Non-ESA Payload Costs - 43 M€

8.1.4 Overall mission cost analysis

Table 8.1 shows a simple comparison between Mars Express and LunarEX. Indeed MEX and LunarEX appear similar in that both involve a planetary orbiter element and a surface element.

From a simple comparison it can be seen that LunarEX costs should be lower than Mars Express.

Table 8.1 Mars Express – LunarEX comparison

Aspect	**Mars Express**	**LunarEX**
Launch Mass (kg)	1223	846
Launcher	Soyuz Fregat	Soyuz Fregat
Mission Duration	>4 years	1 year
Mass of Surface Element	60 kg (33kg Beagle-2)	158kg (4 x 13kg penetrators + descent modules)
Mass of orbiting payload	116kg	0kg
Mass of fuel	426kg	306.4kg
Launch dry mass (i.e. launch mass - fuel)	797kg	539.7kg
ESA Costs (M€)	204	155*
National Costs (M€)	~100	43

*Scaling from 80% launch payload dry weight. Further reductions can be envisaged from reduced operations costs. Note the additional cost of De-orbit and attitude control units is offset by the savings from the absence of an orbiter scientific payload.

The above estimate can be compared with an approximate MoonLITE UK mission cost estimate of 140-160 M€.

9. Communications and Outreach

The Lisbon European Council Meeting in March 2000, in the celebrated “Lisbon Declaration” recognized the important role of education as an integral part of economic and social policies for strengthening Europe’s competitive position worldwide. The meeting set the strategic objective for the European Union to become the world’s most dynamic knowledge-based economy.

However in summing up the outcome of the recent Space Education Forum held in June, 2007 at the international Space Science Institute in Bern, the Executive Director Professor Roger M. Bonnet remarked “that the aims of the Lisbon Declaration are pursued energetically in the USA but apparently no longer in Europe”

Europe is critically short of young scientists and engineers. Of all the domains that have the potential to inspire, Space remains at the forefront.

Within the Space domain, planetary science and exploration is probably the most engaging to the public.

LunarEX has the potential to be a very high profile mission. It will be novel and exciting and will take place at a time when Lunar exploration has re-emerged in the public eye. A general sense of 'Man returning to the Moon' is growing and we can expect to see a dramatic increase in interest. This will improve public awareness of the issues that the mission seeks to address (origin of the Earth, implications of water ice on potential for manned planetary exploration and the origin of life).

The relatively short duration of the first phase will include a number of significant events (Launch, orbit insertion, four surface deployments and four 'first light's plus potential water discovery and, later Lunar core discovery) which should maintain public interest and media coverage. While comparisons with Apollo will be made, it will also be noted that at least two penetrators will impact in locations which were not accessible to Apollo (Far Side and shaded craters): thus it will be easy to communicate significant advances being made by LunarEX.

Within this context it is proposed to plan an outreach programme linked to key mission milestones. Live coverage of impacts and first transmission is a strong possibility since through ESA ownership, confidence will be very high. Descent images transmitted in near real time will be reminiscent of the first Ranger photographs.

Moreover, the high technology, and apparently highly challenging nature of the penetrator concept offers a showcase for European technology.

10. References

Church, P., QinetiQ, LunarEX study report June 2007

Chyba, C.F., Sagan, C. Endogenous production, exogenous delivery and impact-shock synthesis of organic molecules: an inventory for the origins of life. *Nature*, 355, 125-132, (1992).

Crawford, I.A. *Space Policy* 20, 91-97, (2004).

Crawford, I.A. *Internat. J. Astrobiol.,* 5, 191-197, (2006)

Feldman, W.C., et al. Fluxes of fast and epithermal neutrons from Lunar Prospector: evidence for water ice at the Lunar poles. *Science*, 281, 1496-1500, (1998).

Fulchignoni, M., Ferri, F., Angrilli, F., Bar-Nun, A., Barucci, M.A., Bianchini, G., Borucki, W. , Coradini, M., Coustenis, A., Falkner, P., Flamini, E., Grard, R., Hamelin, M., Harri, A.M., Leppelmeier, G.W., Lopez-Moreno, J.J., McDonnell, J.A.M., McKay, C.P., Neubauer, F.H., Pedersen, A., Picardi, G., Pirronello, V., Rodrigo, R., Schwingenschuh, K., Seiff, A., Svedhem, H., Vanzani, V., Zarnecki J., (2002). The Characterisation of Titan's Atmospheric Physical Properties by the Huygens Atmospheric Structure Instrument (Hasi) *Space Science Review*s, **104** (1) 395-431

Gao, Y, A. Phipps, M. Taylor, J. Clemmet, D. Parker, I. A. Crawford, A. J. Ball, L. Wilson, A. Curiel, P. Davies, M. Sweeting, A. Baker, "UK Lunar Science Missions: MoonLITE & Moonraker", *Proc. DGLR Int. Symposium "To Moon and beyond"*, Bremen, Germany, March, 2007

Gao, Y. and Phipps A., ESA Cosmic Vision Proposal LunarEX, V.2, June 2007.

Goins, N.R., Dainty, A.M., Toksoz, M.N. Lunar seismology – the internal structure of the Moon, *J. Geophys. Res*. 86, 5061-5074, (1981).

Griffiths, A.D., Coates, A..J., Jaumann, R., Michaelis, H., Paar, G., Barnes, D., Josset, J.-L., and the PanCam team, Context for the ESA ExoMars Rover: the Panoramic Camera (PanCam) Instrument, International Journal of Astrobiology, doi:10.1017/S1473550406003387, 2006.

Hagermann, A. and Tanaka, S. Ejecta deposit thickness, heat-flow, and a critical ambiguity on the Moon. *Geophys. Res. Lett.*, 33, L19203, (2006).

Jolliff, B.L., Gillis, J.J., Haskin, L.A., Korotev, R.L., Wieczorek, M.A. Major Lunar crustal terranes: surface expressions and crust-mantle origins. *J. Geophys. Res*. 105(E2): 4197-4216, (2000).

Khan, A. An inquiry into the Lunar interior – a non-linear inversion of the Apollo seismic data. *J. Geophys. Res*, 107, 1-23, (2002).

Langseth, M.G. et al. *Lunar Planet. Sci. Conf*., 7, 3143-3171, (1976).

Lognonné, P. Planetary Seismology, *Ann. Rev. Earth. Planet. Sci*., 33, 571-604, (2005).

Lognonné. P., et al. A new seismic model of the Moon: implications for structure, thermal evolution and formation of the Moon. *Earth. Planet. Sci. Lett*., 211, 27-44, (2003).

Lucey, P.G. Potential for prebiotic chemistry at the poles of the Moon. *Proc. SPIE*, 4137, 84-88, (2000).

May, R. D. and C.R. Webster, Data-processing and calibration for uneable diode-laser harmonic absorption spectrometer, J. Quant. Spectrosc. Radiant. Transfer, 49, 335-347, 1993.

Tanaka, S., Yoshida, S., Hayakawa, M., Horai, K., Fujimura, A., and Mizutani, H., Development of the heat flow measurement system by the Lunar-A penetrators, Adv. Space Res. 23, pp1825-1828, 1999.

Tanaka, S., Yoshida, S., Hayakawa, M., Fujimura, A., and Mizutani, H., Thermal Model of the Lunar-A Penetrator and its effect on the accuracy for Lunar heat flow experiment, Proc. Fourth Int. Conf. on the Exploration and Utilization of the Moon, July 2000, (ESA SP-462).

Mizutani, H., Fujimura, A., Tanaka, S., Shiraishi, H., Nakjima, T., 'Lunar-A mission: Outline and current status', J. Earth Syst. Sci., 114, No 6, Dec 2005, pp 763 – 768.

Nakamura, Y., et al. Shallow Moonquakes: depth, distribution and implications as to the present state of the Lunar interior. *Proc. Lunar Planet. Conf.*, 10, 2299-2309, (1979).

Nakamura, Y., Seismic velocity structure of the Lunar mantle, *J. Geophys. Res.* **88** (1983), pp. 677–686, 1983.

Neal. C.R. The importance of establishing a global Lunar seismic network. Paper presented at the 2005 Space Resources Roundtable, Abstract #2065, (2005).

NRC. *The Scientific Context for Exploration of the Moon - Final Report*, National Research Council, Washington D.C, (2007)

Overmaat, T, Optimisation of a Lateral Capacitive Array Transducer *M. Sc. Thesis*, Imperial College London (2005)

Pierazzo, E., Chyba, C.F. Amino acid survival in large cometary impacts. *Meteorit. Planet. Sci*., 34, 909-918, (1999).

Pike W. T., Karl W., Kumar, S. Vijendran S., Semple T (2004) Analysis of sidewall quality in through-wafer deep reactive-ion etching, *Microelectr. Engng*. **73-74**, 340

Pike, W. T. and I. M. Standley, (2005) Determination of the dynamics of micromachined lateral suspensions in the scanning electron microscope J. *Micromech. Microeng.* **15** S82-S88

Pike W.T., Standley, I.M. and Syms, R. R. A. (2006) Micromachined Accelerometer *U.S. Patent* 7,036,374

Potts, P.J.; Webb, P.C.; Williams-Thorpe, O.; Kilworth, R. Analysis of silicate rocks using field-portable X-ray fluorescence instrumentation incorporating a mercury (II) iodide detector. Analyst 1995, 120 (5), 1273–1278.

Rieder, R., T. Economou, H. Wänke, A. Turkevich, J. Crisp, J. Bru¨ckner, G. Dreibus, and H. Y. McSween, The chemical composition of Martian soil and rocks returned by the mobile alpha proton x-ray spectrometer: Preliminary results from the x-ray mode, Science, 278, 1771– 1774, 1997.

Seidensticker, K. J., Möhlmann, D., Apathy, I., Schmidt, W. Thiel, K. Arnold, W., Fischer, H.-H., Kretschmer, M., Madlener, D., Péter, A., Trautner, R., Schieke, S. (2007) Sesame - An Experiment of the Rosetta Lander Philae: Objectives and General Design. *Space Science Reviews*, **128** (1) 301-337

Simoes, F., Trautner, R., Grard, R., Hamelin, M., Lebreton, J.-P., CETP, France; (2006) "A Mutual Impedance Probe for Measuring the Dielectric Properties of the Atmosphere and of the Surface of Planetary Environments" *4th International Planetary Probe Workshop*, June 27-30 2006 Pasadena

Sims, M.R., et al. (1999) *Adv. Space Res*., 23, 1925-1928.

Smrekar, S., Catling, D., Lorenz, R., Magalhaes, J., Moersch, J., Morgan, P., Murry, B., Presley, M., Yen, A., Zent, A. and Blaney, D. Deep Space 2: the Mars Microprobe Mission Journal of Geophysical Research, Vol. 104, No. E1 1, Pages 27,013-27,030, November 25, 1999

Spudis, P.D. *The Once and Future Moon*, Smith. Inst. Press, (1996).

Vaniman, D., et al. The Lunar environment. In: *The Lunar Sourcebook*, CUP, pp. 27-60, (1991).

Todd, J.F.J., Barber, S.J., Wright, I.P., Morgan, G.H., Morse, A.D., Sheridan, S., Leese, M.R., Maynard, J.M., Evans, S.T., Pillinger, C.T., Drummond, D.L., Heys, S.C., Huq, S.E., Kent, B.J., Sawyer, E.C., Whalley, M.S., and Waltham, N.R. (2007) Ion trap mass spectrometry on a comet nucleus: the Ptolemy instrument and the Rosetta space mission. *Journal Of Mass Spectrometry* **42** (1): pp 1-10

Trotignon, J. G., Michau, J. L., Lagoutte, D., Chabassière, M., Chalumeau, G., Colin, F., Décréau, P. M. E., Geiswiller, J., Gille, P., Grard, R., Hachemi, T., Hamelin, M., Eriksson, A., Laakso, H., Lebreton, J. P., Mazelle, C., Randriamboarison, O., Schmidt, W., Smit, A., Telljohann, U., Zamora P., (2007) RPC-MIP: the Mutual Impedance Probe of the Rosetta Plasma Consortium. *Space Science Reviews*, **128** (1) 713-728.

Vaniman, D., et al. The Lunar environment. In: *The Lunar Sourcebook*, CUP, pp 27-60, 1991.

Wells, N., LunarEX Penetrator Power and Communications Study Technical Note. Issue 1, QinetiQ, 01-June-2007.

Wieczorek, M. A and Phillips, R. J. *J. Geophys. Res*., 105(E8) 20,417-20,430, (2000).

Wieczorek, M.A., et al., New Views of the Moon, *Rev. Min. Geochem*., 60, 221-364, (2006).

Wright, I.P., Barber, S.J., Morgan, G.H., Morse, A.D., Sheridan, S., Andrews, D.J., Maynard, J.M., Yau, D., Evans, S.T., Leese, M.R., Zarnecki, J.C., Kent, B.J., Waltham, N.R., Whalley, M.S., Heys, S.C., Drummond, D.L., Edeson, R.L., Sawyer, E.C., Turner, R.F. and Pillinger, C.T. (2007) Ptolemy – an Instrument to Measure Stable Isotopic Ratios of Key Volatiles on a Cometary Nucleus. *Space Science Reviews **128** No. 1-4 / Feb.2007 pp. 363-381*